공학석사 학위논문

Multifunctional Graphene Liquid Crystal Fibers and Their Fabric Devices

다기능성 그래핀 액정 섬유제조 및 섬유소자 연구

2017 년 8 월

서울대학교 융합과학기술대학원

융합과학부 나노융합전공

김 혁 준

Multifunctional Graphene Liquid Crystal Fibers and Their Fabric Devices

Hyuk Joon Kim

Program in Nano Science and Technology

The Graduate School of Convergence Science and Technology

Seoul National University

As the performance of portable electronic devices has been improved and multi-functions have been demanded, development of electric energy storage technology and flexible electronic materials has become very important recently. So smart textile for the manufacture of wearable electronics / devices has been come up for. Due to the smart textile, studies on multifunctional new materials are attracting attention and graphene is especially getting more attention for their physical and electrical properties.

The graphene oxide exhibits liquid crystal properties due to the plate-like particles and has orientational order provoking isotropic-nematic phase transition above the critical concentration. Using these properties, it became possible to fabricate graphene oxide fibers with wet spinning. Graphene's fiberization technology has a textile characterization of 1D material, which was impossible with film-like flexible elements, which are conventional 2D materials. The fiberization of graphene has been specialized in wearable materials and devices as it becomes possible to knot, twist, weave, and sew.

In this study, the graphene oxide liquid crystal properties were investigated and the characteristics of graphene oxide fiber were analyzed by the reduction mechanism. The isotropic-nematic phase transition of graphene oxide liquid crystals was confirmed by cross-polarized image and diameter dispersion analysis according to graphene oxide particle size. Particularly, particles in the range of 50-100 μm were found to have a large influence on nematic properties. Graphene oxide fibers were fabricated by wet spinning using graphene oxide liquid crystal, and the characteristics of the fibers were compared and analyzed according to the change of HI / AcOH reducing agent concentration. The increase of the density was deduced from the reduction of the fiber diameter due to the reduction of the reducing agent concentration, which was confirmed to lead to an increase in the mechanical strength. In the electrical conductivity measurement, the electrical conductivity of the low density (10% HI / AcOH) reduced fiber was about 2 times higher than that of

the high density (30% HI / AcOH) reduced fiber. It can be expected that the graphitic properties have been effectively restored. In particular, the electrochemical measurement results showed that the low-density-reduced fibers exhibited higher energy storage characteristics ($211Fg^{-1}$ and $167Fg^{-1}$, respectively) than the high concentration, and the output density was about 77% higher. These facts suggest that the pathway of the reduction products depends on the HI concentration and that the reduction products may greatly affect the properties of the reduced graphene oxide fibers with or without double bond recovery.

From these results, we propose optimization conditions of graphene oxide fiber by securing the characteristics of graphene oxide liquid crystal and establishing reducing agent reducing conditions.

Keywords: Graphene, Graphene liquid crystal fiber, wet-spinning, Energy storage devices, Flexible devices

Contents

List of Tables

List of Figures

1. Introduction

1.1 Motivation

The development of electric energy storage technology and flexible electronic materials has become very important recently as the performance of portable electronic devices has improved and more functions are required. Among them, wearable devices / electronics started with head mounted devices (HMDs), which were proposed by MIT researchers in the 1960s, and opened up possibilities of flexible electronic materials through flexible displays developed by Xerox in the 1970s. After that, studies for securing the flexibility and performance of substrates and devices have been actively conducted. In 2010, smart watches and bracelet-type wearable devices started to be mass produced. However, the function of the currently produced wearable devices is very limited, and not a few of the device is still made of a non-flexible material. Accordingly, a smart textile including a film type, a fiber type, and a sponge type material is being considered as a concept for manufacturing an ergonomic wearable electronic device. Smart fabric materials require fundamental performances such as thermal conductivity, electrical conductivity, flexibility, and electrochemical characteristics, and therefore research on multifunctional new materials is attracting attention.[1]

Graphene fibers are known to be the most likely material to implement smart fabrics. Grafin's fiberization technology has a textile characterization of 1D material, which was impossible with film-like flexible elements, which are conventional 2D materials. Conventional flexible film materials are highly adhesive to the polymer film, so they are presented as adhesive materials. However, the fiberization of graphene is known to be more suitable for wearable materials and devices as it becomes possible to knot, twist, weave, and sew.[2,3,4] Carbon nanotube (CNT) fiber which is presented as a typical carbon fiber materials with graphene has excellent electrical conductivity, but has low energy storage characteristics (5 Fg^{-1}) and has a very high production cost, which limits commercialization. On the other hand, graphene fibers have been proved to have excellent industrial value as a material of high sensitivity sensor and energy storage of fiber type because graphene fibers have excellent specific surface area (~2600 m^2g^{-1}). Therefore, studies using graphene fibers have been actively conducted on functional fabric type electronic devices such as energy storage devices, gas sensors, and motion sensors.

The reduction process in the process of graphene oxide fibers is a very important process for producing reduced graphene oxide (RGO) fibers from graphene oxide. However, currently known methods require a high temperature heat treatment

(~1000 ℃) for a sufficient reduction of graphene oxide, or 24 hours for chemical methods. Especially, various studies have adopted the chemical reduction method but the experimental conditions are different from each other and the basis of the reduction principle is insufficient. Therefore, optimization of the chemical reduction process is required.

In this study, the graphene liquid crystal solution is used to fabricate the graphene oxide fiber, and the electrical / electrochemical characteristics and mechanism of the graphene liquid crystal fiber which is reduced according to the reduction conditions are presented.

1.2 Graphene oxide liquid crystal

1.2.1 Properties of graphene and graphene oxide

Graphene is a two-dimensional atomic layer material with a hexagonal carbon ring structure containing a double bond, which indicates a single molecule of about 0.2 nm in thickness constituting graphite. That is, a large number of graphene layers are piled up to form graphite. Graphene is known to have high electrical conductivity, mechanical strength, thermal conductivity, high specific surface area (~2600 m^2g^{-1}), and electrochemical capacitance (~21 $\mu F \cdot cm^{-2}$) due to structural characteristics. Therefore, it is expected that the electrical and electrochemical characteristics will be very excellent, and it is emerged as a multifunctional new material because it has a light density and high surface area efficiency compared with the existing metal materials.

Various graphene fabrication methods have been proposed to utilize the advantages of graphene, and mechanical exfoliation, chemical vapor deposition (CVD), and chemical synthesis have been widely used.[5] However, artificially produced graphene does not meet the intrinsic properties studied theoretically, which is caused by defects that occur during manufacturing. Graphene defects are caused by topological defects, lattice vacancies, adsorption atoms (adatom), etc.[5,6]

The CVD method is a method of growing graphene by precipitating carbon dissolved on a metal surface using a metal as a catalyst, and monolayer graphene can be synthesized in a large area. This method is suitable for producing high-quality graphene with a low defect of graphene and high charge mobility. However, its fabrication condition is complicated and unsuitable for mass production since a very high temperature (~1000℃) and a vacuum condition (10^{-3} torr) are required.[7,8] In the chemical synthesis method, on the other hand, graphene oxide is synthesized by inserting an oxidizing functional group between graphene layers of graphite in a solution and simultaneously peeling the graphene oxide, and reducing it again to form reduced graphene oxide (RGO).[9] In this method, graphene oxide can be obtained from a single layer to an aqueous layer, and mass production is possible through a low-cost solution process. However, structural and physical defects are likely to occur in the manufacturing process. Removal of functional groups and recovery of graphene structure are very important to reduce such defects. Since graphene oxide is easy to process in various forms such as ink, thin film, fiber, and sponge, studies have been reported to reduce defects and enhance graphene properties.

	Graphene	Graphene oxide
Method	CVD	Solution base synthesis
Principle	Vapor deposition	Redox reaction
Condition	High temperature (>1000 ℃), Vacuum (<10^{-3} torr)	Room temperature Atmospheric pressure
Electron mobility ($cm^2V^{-1}s^{-1}$)	4,000	10 (RGO)
Carbon source	CH_4 (gas)	Graphite
Product foam	Thin film	Solution, powder film, fiber…
Defect	(Relatively) Low	(Relatively) Large
Productivity	Only thin film	More than Kg

Table 1. Comparison of graphene and graphene oxide

1.2.2 Graphene oxide liquid crystal properties

Liquid crystal (LC)

Liquid crystal refers to the state of a substance that exhibits intermediate properties between solid and liquid phases. The mesophase, which is formed during the phase transition, has a molecular arrangement similar to that found in solid crystals, although it normally exists as a liquid in nature.[10] Liquid crystals are largely classified into thermotropic and lyotropic. The thermotropic liquid crystal shows a steady state of the mesophase due to the change of heat, whereas the lyotropic liquid crystal appears when the solution concentration exceeds the threshold value. The critical concentration (CC) is the concentration at which the lyophilic liquid crystal appears. When the concentration of the solute is reached, the isotropic characteristic of the liquid is weakened and the mesophase appears due to the orientation of the molecules. Liquid crystals are defined as various kinds of mesophase depending on orientational order and positional order. Table 2 describes the classification of the image according to the structure of the liquid crystal. In the Nematic phase, the long axes of molecules are aligned in parallel, but each molecule moves relatively freely in the major axis direction.

Graphene oxide liquid crystal

The graphene oxide dispersion system exhibits a typical lyotropic liquid crystal. At this time, the mesophase is formed according to the shape, size, solution concentration and viscosity of the graphene oxide particles, and liquid crystals are formed by isotropic–nematic phase transition. Because these factors are complex, particle size and concentration control is required to obtain a graphene oxide dispersion system with a clear nematic phase.[11]

The isotropic–nematic phase transition of a thin plate–like material occurs theoretically above a certain aspect ratio D / δ.[12] δ is the thickness of the plate, and D is the nominal diameter of the plate. The graphene oxide plate phase is assumed to approximate D from the diameter of the circle on the same area because the shape is uneven. This hypothesis is shown in Figure 1. Theoretically, the graphene oxide solution has a biphasic state at an aspect ratio of 600 or more and the transition begins to appear. In general, graphene or graphene oxide, which is well separated from graphite, shows little difference in thickness. As a result, the aspect ratio of graphene is proportional to the nominal diameter of the particles. Thus, the phase transition of graphene is closely related to the particle size.[12]

At low concentration of graphene oxide dispersion (0.05–0.6wt%), which is sufficiently left for 3 weeks, the two phases are macroscopically separated. The supernatant having a relatively low density exhibits an isotropic phase while the submerged liquid having a high density exhibits a birefringence characteristic when a cross polarization is measured. The lower layer entrained with dark and bright areas showed the structure of the Schlieren texture on a typical nematic. This is a dual phase behavior, in which isotropic phase and nematic phase coexist. The size of the area consisting of the dual phases is due to the polydispersity of the graphene oxide particles. That is, the wider the distribution of graphene oxide particles, the larger the dual phase region.[27]

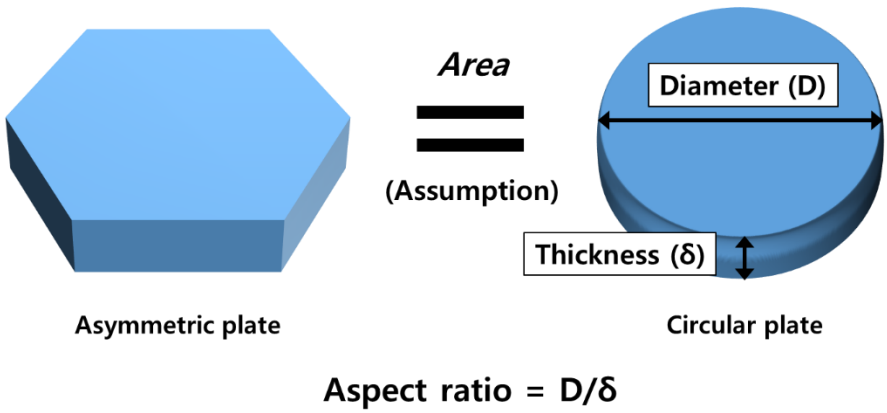

Figure 1. A schematic diagram showing a method for determining the nominal diameter through the assumption of a circular plate for determining the aspect ratio of asymmetric plate-shaped particles.

Even in a graphene oxide liquid crystal having the same degree of oxidation, the critical concentration at which the phase transition occurs varies with the average particle diameter. The graphene oxide dispersion system having an average particle diameter of 1.65 μm has already a complete nematic phase at a concentration of 0.53wt%, whereas a dispersion having an average diameter of 0.75 μm maintains a double phase even when the concentration increases to 0.75wt%. At temperatures above the critical temperature, the nematic phase is maintained until the boiling point is reached.[27]

In the graphene oxide dispersion system of the same concentration, the volume ratio of the nematic phase becomes larger as the D value increases. That is, the larger the graphene oxide particle, the easier the nematic phase is to be seen, and the lower the critical concentration required. As a result of this nematic phase, the graphene oxide dispersion (D~2.1 μm) starts to show Schlieren texture at a concentration of 3 mg · cm^{-3} or more and starts to show a stable nematic phase at from 5 to 8 mg · cm^{-3}. At concentrations above 10 mg · cm^{-3}, high levels of lamellar mesophase are present. From these evidence, it was confirmed that the graphene oxide dispersion system exhibited a liquid–crystal liquid crystal behavior above a certain concentration. [11,13]

Since there is a strong correlation between the particle size and the critical concentration, it is theoretically possible to deduce the isotropic phase and nematic phase transition from the critical volume fraction (φ). The critical volume fraction is determined based on the liquid phase model of the charged plate-like dispersion system.[14]

$$\Phi = \frac{3}{8}\sqrt{3}\frac{L}{D}\frac{1+\partial^2}{1+3\partial^2}\rho D^3 \qquad \text{(Equation 1)}$$

∂ : Polydispersity

L: Thickness of plate

D: Nominal diameter

ρD^3: Number density

This equation is only applied to particle models with a solid and uniform diameter dispersion so it differs somewhat from the experimental data. But it is still possible to deduce the phase transition using the number density (ρD^3) as an index. For example, if the concentration and particle size of the dispersion system are confirmed, the number density regions of the isotropic phase and the nematic phase can be determined, and a

critical concentration region in which the phase transition occurs can be expected.[15,16] The resulting critical concentration values are measured lower than the theoretical values. Graphene oxide is mainly dispersed in pure water, and water is a good polar solvent. Therefore, graphene oxide particles are present in an unfolded state. Electrostatic repulsive forces and irregular shapes of charged surface functional groups also increase the effective area of the particles and reduce the concentration at which phase transitions occur.[27]

The ionic strength and pH also have a great influence on the stabilization of graphene oxide liquid crystals. The electrostatic repulsive force of functional groups such as carboxyl groups plays an important role in the stabilization of graphene oxide. Therefore, when the ionic strength is increased or the pH is lowered to reduce the repulsive force between particles, aggregation of graphene oxide particles occurs. This artificial destabilization can be applied to wet spinning processes to produce fibers from graphene oxide liquid crystals.[27]

	Nematic	Cholesteric	Smetic
Model		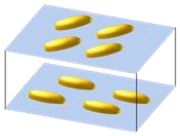	
Oridentational order	O	O	O
Positional order	X	X	O
Layer	X	O	O

Table 2. Phase classification according to liquid crystal structure

1.2.3 Chemical synthesis of graphene oxide

As described above, graphene has a structure with favorable nematic phase because it has a high formation ratio by having a thickness of several micrometers to the atomic level thickness. However, in order to form a liquid crystal, the dispersion degree with respect to the solvent should be considered. Pure graphene is not dispersed in water and hardly dispersed in organic solvents. It is known that the maximum of 10^{-5} wt% of pure graphene is dispersed in typical organic solvent NMP (N-methylpyrrolidone) and only up to 3×10^{-5}wt% is dispersed in ortho-dichlorobenzene. Agglomeration due to strong $\pi-\pi$ overlap between grains of grapheme is the main cause of this. It is therefore impossible to form liquid crystals directly with pure graphene. Chemically oxidized graphene, graphene oxide, is used to solve this problem. The graphene oxide has an aspect ratio similar to that of graphene and has a high dispersion degree to the solvent due to various oxidizing groups on the surface. Oxidizing groups such as hydroxyl(-OH), carboxyl(-COOH), ether(-O-) and epoxy groups cause graphene to be negatively charged, Thereby greatly increasing the dispersion degree for the polar solvent. Graphene oxide can be dispersed in water and various organic solvents to form liquid crystal properties. In addition, graphene oxide is of high value as a multifunctional material because it is capable of imparting additional chemical

properties through doping and forming a complex with other materials. Graphene oxide forms a reduced graphene oxide through an additional reduction process, which has properties similar to graphene. Therefore, it is essential to synthesize graphene oxide in order to secure and utilize liquid crystal properties from graphene.[13]

Table 3 summarizes typical methods for producing graphene oxide. In the synthesis method by Hummer's method, sulfuric acid is inserted into the graphite layer as a solvent and plays a role of promoting the oxidation reaction of the oxidant ($KMnO_4$) added later. $NaNO_3$ enters the graphite layer in an ionic form together with sulfuric acid at the beginning of the reaction and causes efficient exfoliation. $KMnO_4$ is activated by the following reaction.[17,18]

$$KMnO_4 + 3H_2SO_4 \rightarrow K^+ + MnO_3^- + H_3O^+ + 3H_3SO_4^- \quad \text{(Equation 2)}$$

$$MnO_3^- + MnO_4^- \rightarrow Mn_2O_7 \quad \text{(Equation 3)}$$

$$Mn_2O_7 + 2H_2SO_4 \rightarrow 2[MnO_3]^+[HSO_4]^- + H_2O \quad \text{(Equation 4)}$$

$$Mn_2O_7 \rightarrow 2MnO_2 + 3[O] \quad \text{(Equation 5)}$$

Mn_2O_7 is a temperature-sensitive intermediate and is known to explode above 55℃.[19] This phenomenon physically destroys graphene or graphite, reducing the particle size of the product. Therefore, low temperature maintenance is required. The activated MnO2 imparts an oxidizing group to the double bond of the graphene. Oxidizing groups make interlayer repulsive force to cause macroscopic exfoliation.

The H_2O_2 then reacts with the residual oxidant to remove residues as follows.

$$MnO_2 + H_2O_2 + H_2SO_4 \rightarrow MnSO_4 + O_2 + H_2O \quad \text{(Equation 6)}$$

HCl then dissolves impurities including residual metal ions into a form that can be removed later. The prepared graphene oxide solution is purified by various methods such as filtration, centrifugation, and dialysis.

Improved synthesis of graphene oxide is known as a method for reducing defects in graphene oxide. In this method, concentrated sulfuric acid and phosphoric acid are used as a solvent in a ratio of 9:1 to reduce defects generated during the oxidation process. Since the exothermic reaction is suppressed by using phosphoric

acid as a catalyst, no toxic gas is generated and the oxidation degree is higher than the conventional synthesis method. Hexagonal structure of graphene is retained and defects are reduced after reduction. In particular, this method has less influence on the size reduction of the graphene oxide particles and can preserve the liquid crystal properties better than conventional methods.[45]

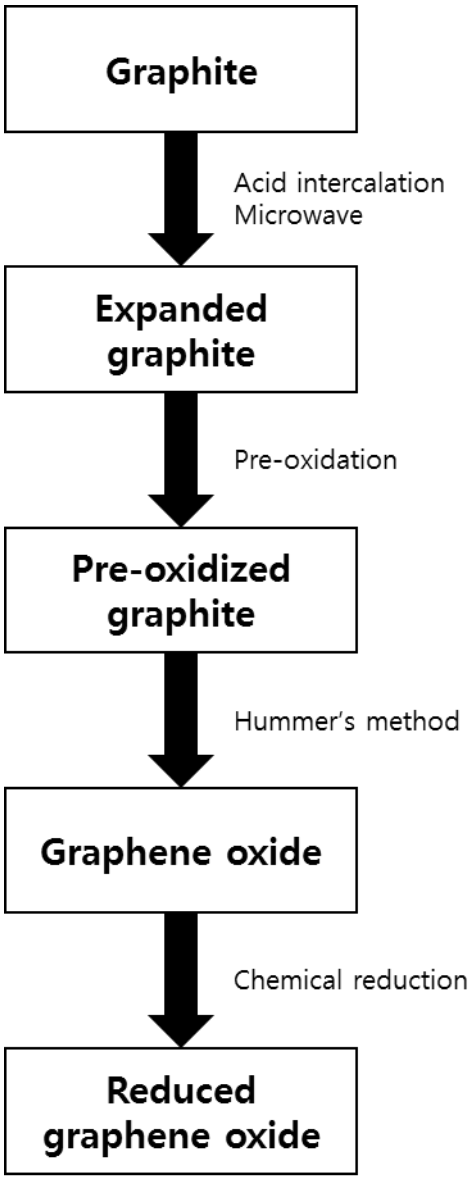

Table 3. Synthesis of reduced graphene oxide.

1.2.4 Synthesis of Graphene Oixde Liquid Crystal

The liquid crystal properties of the graphene oxide are largely influenced by the size of graphene oxide particles as mentioned above. The higher the formation ratio of graphene oxide particles, the lower the concentration of nematic phase. Therefore, in order to maintain the liquid crystal property of the graphene oxide solution, it is necessary to minimize the phenomenon that the particles physically break down and become small.

To maintain the particle size during chemical synthesis, i) the particle size of the reactant (graphite), ii) the reaction environment, and iii) the dispersion method should be considered. First, the size of the graphite, which is a raw material of the graphene oxide as a reactant, can be selected. Graphite particles are inevitably physically destroyed by the processes of peeling and mixing in the oxidation and reduction processes. However, if the particle size of the starting material is large, the size of the synthesized particle is likely to increase.[20] Graphene oxides generated from graphite of a few hundred micrometers in size maintain a size of tens or hundreds of micrometers, while graphite with a size of a few hundreds of nanometers to a few micrometers naturally produces nano-sized crushed particles. Thus, the choice of large grains of graphite plays an important role in the formation of graphene oxide liquid crystals.

Environmental control during graphene oxide synthesis is also important. Graphene oxides are generally synthesized by the Hummer's method where the particles are chemically and physically destroyed during the oxidation and reduction processes. In the oxidation process, it is known that the dissolution heat generated by the addition of the oxidizing agent, the addition of the oxidizing functional groups, the defects generated during the peeling process, and the heat due to the water and the sulfuric acid reaction during the neutralization process all destroy graphene oxide particles. For example, the intermediate reactant of $KMnO_4$ reacts explosively at 55℃ or higher to cause particle fracture. Therefore, it is necessary to control the heat of dissolution and reaction generated when the oxidizing agent is added.[19] In addition, temperature control in the neutralization process is essential. Since the solvent of Hummer's method is sulfuric acid, even when only a very small amount of water is added during neutralization, the reaction is explosive and the temperature rises sharply. This involves explosion of the remaining intermediate reactant (Mn_2O_7) and physical destruction due to internal gas evolution. Therefore, temperature control of the neutralization process is a key factor for maintaining graphene oxide particle size. The reduction process is affected by the reactivity and temperature of the reagents. Reagents such as $NaBH_4$ and N_2H_4 generate

considerable gas due to excessive reactivity and heat. This destroys graphene oxide particles at the macroscopic point. The graphene oxide film was observed to be destroyed by the intense reaction of the two reagents.[21] Similarly, it has been reported that graphene oxides reduced at a temperature of 50℃ or higher under reducing conditions are defective due to gasification (CO_2) of functional groups.[6] Through the examples presented, it can be seen that maintaining the temperature during oxidation and reduction is an essential process for maintaining the liquid crystal properties of graphene oxide.

On the other hand, in past studies, ultrasonic dispersion was used in the process of producing graphene oxide solution. However, it has been confirmed that ultrasonic dispersion disrupts graphene oxide and the particle size is greatly reduced. Thus, it is confirmed that it is not suitable for producing graphene oxide liquid crystal.[22] In particular, the graphene oxide solution after ultrasonic dispersion for 1 hour decreased from an average diameter of 10 μm to several hundred nanometers.[23]

In addition to the three factors such as the particle size of the starting material, the reaction environment, and the ultrasonic dispersion, pH neutralization and impurity removal through neutralization ensure that the graphene oxide particle size and dispersion are uniformly sized to form a nematic phase. When the solvent of graphene oxide has a low pH, agglomeration between

particles occurs due to the nature of acid ions. Oxidizing groups on graphene oxide cause the particles to become negatively charged. This causes a repulsive force between the particles to prevent the particles from accumulating and to be dispersed well in the polar solvent. However, when the particles are in an acidic environment, they are surrounded by positively charged particles such as hydrogen ions (H^+) and the repulsive force between particles is reduced. The functional group capable of hydrogen bonding with the polar solvent molecule is surrounded by the hydrogen ion, so that the interaction with the solvent is reduced and dispersion becomes impossible. As a result, aggregation or precipitation occurs. A high pH environment, i.e., a basic solvent, also interferes with the dispersion of the graphene oxide. The solvent is saturated by the basic ion and the solvation of the graphene oxide is inhibited and the dispersity is lowered. That is, in an excessively high or low pH environment, the graphene oxide is not dispersed in the solvent, which means that the liquid crystal property cannot be exhibited. Therefore, sufficient neutralization of the solution is required.

Impurities and particle size distribution also affect liquid crystal formation. When the particle size distribution is large, particles with large diameters will interfere with each other in particle orientation. As the particle distribution increases, it cannot form a lamellar structure, and it becomes difficult to have a nematic

phase. Impurities also inhibit the possibility of forming liquid crystals on a similar principle. Therefore, in order to secure the liquid crystal, uniformity of the particle diameter and removal of impurities must be accompanied.

These facts suggest that the use of large particles of graphite, temperature control during synthesis and reduction, dispersion of solution excluding ultrasound, neutralization process and particle homogenization are key technologies for producing graphene oxide liquid crystals.

1.3 Graphene oxide liquid crystal fiber

1.3.1 The principle of wet spinning

Wet spinning is a method of dissolving a polymer in an appropriate solvent to make a spinning solution, extruding it through a spinneret in a coagulation solution, and solidifying the polymer to produce a fiber. In order to fabricate graphene oxide fibers through wet spinning, graphene oxide doping, injection rate, nozzle particle size, and the type and concentration of coagulation above a critical concentration should be considered.[24]

During the process of injecting the graphene oxide dispersion into the coagulation solution through the nozzle, gelation of the graphene oxide occurs to form the graphene oxide gel fiber. This process is illustrated in the schematic diagram in Figure 2. When the dispersion is injected, a capillary force is generated by passing through the nozzle and aligns the graphene oxide liquid crystal in the shear direction. The aligned liquid crystal solution is ejected out of the nozzle and comes into contact with the coagulation solution to cause solvent exchange. In this process, ion or solvent penetrates into the graphene oxide liquid crystal, so that the partial negative charge of the graphene oxide is canceled and the repulsion force between particles is reduced and cross-linking occurs. The solvent-displaced graphene

oxide liquid crystals solidify to form graphene oxide gel fibers.[25,26]

The liquid phase is an essential material prior to the production of graphene oxide fibers. Liquid crystal radiation causes structural alignment to occur during the process of radiating the dope to the fibers. The spinnability of graphene oxide liquid crystals depends on the size of the graphene oxide particles and the concentration of the solution. Rugged graphene oxide gel fibers are fabricated only in graphene oxide dope in a state of mesophase. Given a homogeneous size of graphene oxide dispersion, the dope should be above the critical concentration. When the size of the graphene oxide particle is small, the critical concentration of the dope required for spinning increases sharply, leading to an increase in viscosity, and a solution having spinning properties cannot be produced. Experimental results show that interfacial interaction (van der Waals force, hydrogen bonding, etc.) strongly acts on grains having an aspect ratio of 104 or more, which enables continuous spinning of graphene oxide fibers. When the thickness of the graphene single layer is assumed to be 0.2nm, a nematic phase starts to appear at a diameter of 120nm or more, and continuous formation of graphene oxide fibers becomes possible at a thickness of 2μm or more. Below the critical concentration, graphene oxide particles become discontinuous and separate. Therefore, a dope

with a critical concentration corresponding to the particle size is required for grapheme oxide fiber fabrication. When a graphene oxide liquid crystal solution having an average diameter of 37 μm was tested at a concentration of 0.1−5.0 mg · mL^{-1}, it was confirmed that a nematic phase appeared from 0.25mg · mL^{-1}. Wet spinning at a density of less than 0.25 mg · mL^{-1} showing an isotropic phase resulted in the fibers not spinning but spreading. At the concentration of 0.25−0.75 mg · mL^{-1}, the isotropic−nematic phase coexists and the graphene oxide gel fibers are partially shortened. Above 0.75 mg · mL^{-1}, the nematic phase is visible in general, and continuous irradiation is possible from this point. This fiber spinning property remained similar up to 5 mg · mL^{-1}.[14]

The polarized image of the gelated graphene oxide fibers exhibits birefringent properties, which means that initially highly ordered graphene oxide domains are retained in the early stages of the emissive process. Graphene oxide does not form a single region unless external forces are applied. However, shear stresses created by graphene oxide particles cause macroscopic alignment within seconds. Due to the large graphene oxide platelets that form large areas, shear stresses occur, which causes macroscopic alignment to occur within a few seconds. Liquid crystals that occupy a larger area are known to yield macroscopic materials with much finer structure and superior

properties. In addition, the applied tension through the spinneret directs the liquid crystal region and fast coagulation preserves this direction. The morphology of the cross-sections in the dried fibers shows that the graphene oxides are laminated and oriented in the fiber axis direction.[14]

The diameter of the nozzle affects not only the alignment of the graphene oxide particles but also the shear rate. Shear rate ultimately affects fiber diameter and spinning speed. It has been reported that nozzles of 34G to 21G (corresponding to diameters of 0.08 to 0.51mm) can be applied in various ways when fabricating graphene oxide fibers.[25]

The choice of the coagulation solution in wet spinning also plays an important role in determining the properties of the graphene oxide fiber. The graphene oxide dispersion solution is stably dispersed in water in the state that the particles are negatively charged. In order to produce fibers, the stable dispersion state must be broken and precipitated in the form of gel or dry fibers. Precipitation through a coagulation solution includes precipitation using a non-solvent, destabilization using an acid, a base, and a salt, neutralization using a counter ion, coagulation through cross-linking, and freeze-drying at a low temperature.[26] By the rule of "like-dissolves-like", the oxygen functionality of graphene oxide with abundant polarity dissolves in a polar solvent or a hydrogen-bondable solvent such as water,

dimethylformamide (DMF), acetonitrile (CH3CN), and tetrahydrofuran (THF). Conversely, non-polar or non-hydrogen bonding solvents precipitates graphene oxide. Solutions of acids, bases, and salts will precipitate excess ions by penetrating into the graphene oxide dispersion to break the dispersion stable state.[14] Amphiphilic, positively charged polymeric ions, divalent cations (Ca^{2+}, Cu^{2+}, Mg^{2+}) can be used as coagulation materials for graphene oxide due to the negative charge on graphene oxide. It is known that the coagulation solution affects the cross-linking of graphene oxide particles and affects the mechanical strength of the fibers. Various substances such as ionic materials like $CaCl_2$, NaOH, KOH, NaCl, and H_2SO_4, polymer materials like chitosan and CTAB (cetyltrimethylammonium bromide), and organic solvents like acetone have been tested. In general, when cationic and polymeric materials were used, the mechanical strength of the fibers was high. The cationic size was small and penetrated into the gel, while the polymer was found to stay on the surface. In the basic solution, the oxygen functional groups of the graphene oxide gel fibers are partially reduced, resulting in loss of hydrogen bonding ability, breaking of interlayer cross-linking, and weakening the mechanical strength. Therefore, the appropriate coagulation solution should be selected and tested considering the strength and the use of the graphene oxide fiber.

The diameter of the dried graphene oxide fibers after wet spinning shrinks to 1/3 to 1/10 of the gel fiber thickness. This means that the coagulation solution occupies 67 to 90% of the volume of the gel fiber. The graphene oxide particles are composed of a layered structure horizontally arranged on the fiber axis, so that the liquid can be isolated between the particle layers. Therefore graphene oxide particles are wrinkled or folded to fill the void during the drying process, creating a passage the steam can escape. Due to this principle, the surface of wet-spun graphene oxide fibers is not smooth after drying and wrinkles are formed along the fiber axis. This folding occurs during the process of forming graphene oxide gel fibers, and a clear pattern appears after drying. Even if the polymer is added or reduced, it retains its structure and leaves wrinkles. The larger the size of graphene oxide particles is, the more wrinkles are formed to effectively remove residual vapors, and the surface structure of the fibers appears to be unbalanced. If the particle diameter is reduced to 100 nm, the cross-sectional shape of the fiber is close to circular.[44]

The grain size of graphene oxide is closely related to the mechanical strength of the fibers produced. As a result of wet spinning of dope composed of average particle diameter of 22 μm and dope composed of 9 μm under the same conditions, both

mechanical strength and elongation were high in graphene oxide fiber with large diameter. Graphene oxide fibers with large particle diameters are flexible and strong enough to be twisted or tied.[43]

It was found that the drawing rate of pulling the fibers in the wet spinning process also affected the structure of the graphene oxide fibers. Non-drawn fibers exhibit an unbalanced cross-sectional shape. However, the cross section of the fiber begins to form the circular shape since the drawing rate is higher than 1.09. It is possible to have a circular uniform cross-sectional shape because the coagulation rate increases by decreasing the stiffness gradient between the surface first coagulated by the softening and the center of the fiber. As the drawing rate increases, the cross-sectional shape becomes increasingly flat and changes to thin film form above 1.82 speed. At low drawing rates, graphene oxide particles are arranged in random directions, and in some cases the entire layer is folded. However, as the drawing rate increases, the particles orient in one direction to form a horizontal graphene oxide layer. Such an increase in orientation means an increase in mechanical strength, which means that a strong fiber can be produced as the drawing rate increases.[43]

The nozzles and the coagulation solution in combination affect the porosity of the graphene oxide fibers. When liquid nitrogen

is used as the coagulation solution, graphene aerogel fibers can be produced. In this case, the shells are accumulated in a densely packed state, and pores are arranged horizontally on the fiber axis in the central portion. These porous graphene oxide fibers are arranged in the axial direction of the fibers due to their liquid crystal properties and have a high specific surface area of 884 m^2g^{-1} together with a high tensile strength (188 $kNm \cdot kg^{-1}$), even though the core and the edge are separated.[11] The porosity in the fiber can be controlled by the coagulation solution and the nozzle, and various materials can be applied using the pores.

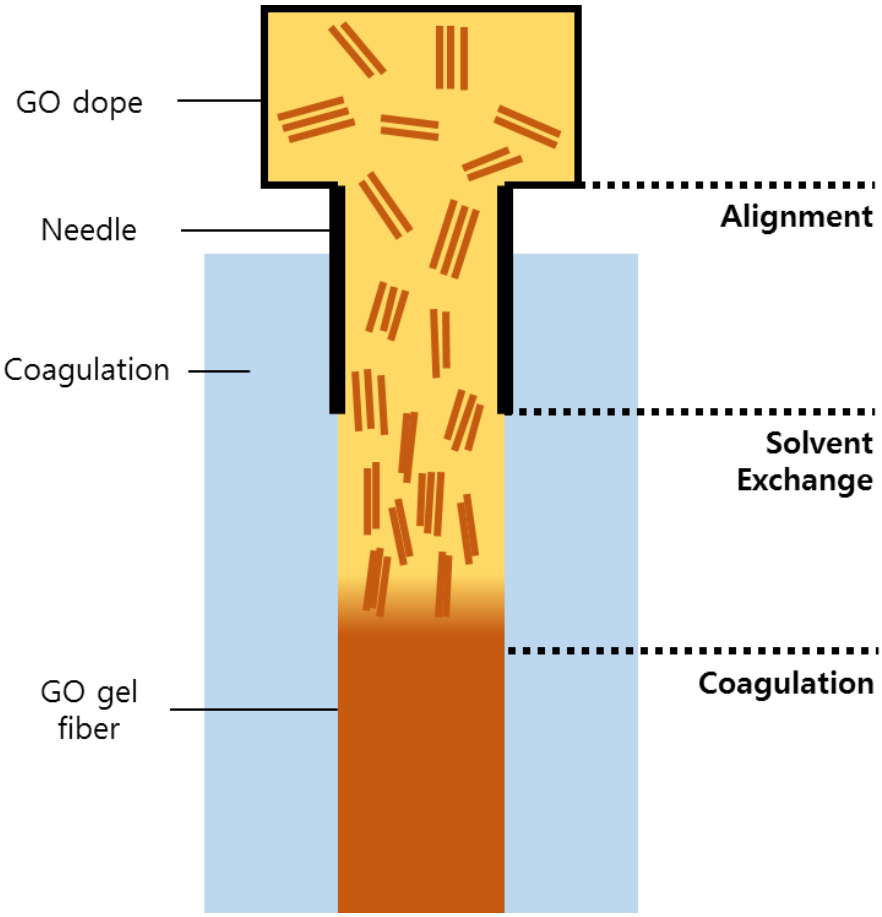

Figure 2. Mechanism diagram in which liquid crystal transitions into fiber form during wet spinning.

1.3.2 Preparation of reduced graphene oxide

Reduction of functional groups is required to restore the properties of graphene from graphene oxide. The main oxidizing groups present on the graphene oxide are typically hydroxyl groups, carboxyl groups, ethers, epoxies, and ketones. When the oxidizing group is reduced, it forms a $\pi-\pi$ double bond of graphene to restore the inherent electrical conductivity and electron mobility.[18,28]

The graphene oxide reduction method is typically a thermal, electrochemical, and chemical reduction method. During the thermal reduction, when heated at a temperature of 800℃ or higher in H_2/Ar (1:9vol%), hydrogen gas is catalyzed and oxidizing groups present on the graphene oxide are reduced.[29,30,31] In the case of chemical reduction, a reducing reagent is used to remove the oxidizing group and restore the carbon-carbon double bond to recover graphene characteristics.

Measures to determine the degree of reduction of graphene include C/O ratio (carbon and oxygen composition ratio) through XPS analysis, ID/IG ratio (D band and G band intensity ratio) measurement using Raman spectroscopy, and electrical conductivity measurement. The C/O ratio of graphene oxide differs depending on the method of preparation of the sample, but it usually ranges from 2 to 4. Reduced graphene oxides that have

undergone chemical reduction generally have a C/O ratio of at least 12 or more, and have been reported up to 246.[32,33,34]

At present, the most widely used reduction method is chemical method. Representative reagents are sodium borohydride ($NaBH_4$), hydrazine (N_2H_4), ascorbic acid (AA) and hydroiodide (HI). $NaBH_4$ is known to be an effective reducing agent for the synthesis of metal nanoparticles, but it is rapidly degraded in aqueous solution and has a short duration (less than 2 hours). So it is highly unsuitable for graphene oxide reduction due to high hydrogen loss.[35,36] AA is eco-friendly and inexpensive, but the reduction efficiency is low due to the weak reduction characteristics.[37] The electrical conductivities of the graphenes reduced to $NaBH_4$ and AA were respectively 82 $S \cdot m^{-1}$ and 800 $S \cdot m^{-1}$. It can be seen that the graphene characteristics are not largely recovered. N_2H_4 is a strong reducing agent with a high degree of reduction (C/O >10.3). The electrical conductivity of the reduced graphene is 2420 $S \cdot m^{-1}$, which is similar to that of graphite, but the toxicity is very strong and a large amount of nitrogen component remains after the reaction.[38] In addition, it has been confirmed that the product gas generated during the reaction process physically destroys the graphene oxide in the film and fiber form, which is inadequate for reduction.

HI is a reagent widely used for the reduction of graphene oxide film and fiber at present (29,800 $S \cdot m^{-1}$) because of its excellent

reducing ability (C/O=12) and excellent conductivity of the product. It is known to bring about similar reductions in organic reactions through electrophilic addition and nucleophilic substitution, which are characteristic of halogen acids. In particular, I^- of HI is most strongly nucleophilic among halogen ions and can effectively lead to a unimolecular nucleophilic reaction (Sn1) and a bimolecular nucleophilic reaction (Sn2) pathway. The epoxide ring is effectively opened and replaced with a hydroxyl group, which is reduced again to recover graphene double bonds. It is also known that when acetic acid is used in combination, it can be reduced at a low temperature of 40℃. ($NaBH_4$ 80℃, N_2H_4 100℃ respectively) by lowering the activation energy through catalysis.

For this reason, many studies have adopted HI / AcOH as a graphene oxide reductant, but the reduction concentration and temperature are varied, and the conductivity is much lower than the high C/O ratio. It does not seem to take account of the reduction mechanism of HI and the occurrence of defects due to heat treatment.

HI reduces oxidizing groups of the graphene oxide through the addition reaction and the substitution reaction as described above. Reduction of the hydroxyl group (−OH) begins when the oxygen atom receives hydrogen and the iodide ion (I^-) is produced. The hydroxyl groups are easily hydrogenated due to the acidic

environment of HI / AcOH and converted into a good leaving group, $-OH_2^+$. This functional group is displaced by iodine by a nucleophilic substitution reaction, leaving off and producing water molecules. Nucleophilic substitution is possible because the nucleophilicity of I^- is 105 times higher than the nucleophilicity of $-H_2O$, although the leaving group ability is similar to pKa = −10 of R−I and pKa = −1.7 of $R-OH_2^+$. Also, since the carbon in the graphene structure with an oxidized group is generally a tertiary carbon, there is a high possibility of leaving $-OH_2^+$ in consideration of stability of carbocation and steric hindrance. Considering the electron affinity of iodine, the steric hindrance of carbon, and the stability of carbon cationization, the mechanism undergoes a mononucleophilic substitution reaction (Sn1).

The iodinated (−I) graphene reacts with HI to produce the final product, where the path of the reaction depends on the concentration of HI. At high concentrations of HI, hydrogen is added to the iodine site and the reaction is completed (Figure 3, Product 2). The bond of the substitution site carbon is sp^3 hybridized state, and the structure before and after reduction has the same structure. On the other hand, in a low concentration HI environment, a double bond is formed in the iodine site to recover the hexagonal carbon ring of the complete grapheme. (FIG. 3, product 3) When the substituent concentration is low, electrons

of the carbon remain in an unsaturated state to form sp^2 hybridization and form a double bond. Product 2 and product 3 from HI concentration have completely different structure, which is very important. Both products result in a similar reduction in the C/O ratio through removal of the oxidizing group, but the electrical conductivity and electron mobility increase only in product 3, which is capable of double bond resonance in the ring. Therefore, product 2 and product 3 have completely different properties, and it can be said that substantially only product 3 has recovered the properties of graphene. As mentioned above, since the reduction conditions of HI / AcOH in many papers are different, the reduction results of graphene oxide cannot be compared with the C/O ratio alone.

The ether and epoxide are also subjected to the hydrogenation reaction and the substitution reaction described above and have a hydroxyl group or an iodine group as an intermediate. The subsequent reaction proceeds identically from the reactant 1 (hydroxyl group) in Figure 3, and the final product is determined depending on the concentration of HI as described above. Therefore, for the precise meaning of reduced graphene oxide fiber fabrication, understanding the reduction mechanism of HI and optimizing the conditions are required.

Reductant	C/O ratio	Condition	Electrical conductivity (S m-1)	Ref.
$NaBH_4$	4.8	80 ℃, 1h	82	[42]
	8.6	R.T., 2h	45	[35]
N_2H_4	10.3	100 ℃, 24h	2420	[38]
Ascorbic acid	-	R.T., 48h	800	[37]
HI	12	100 ℃, 1h	29,800	[21]
HI / AcOH	11.5	40 ℃, 40h	30,400	[39]

Table 4. Typical types of reducing agents and properties of their reduced graphene oxides.

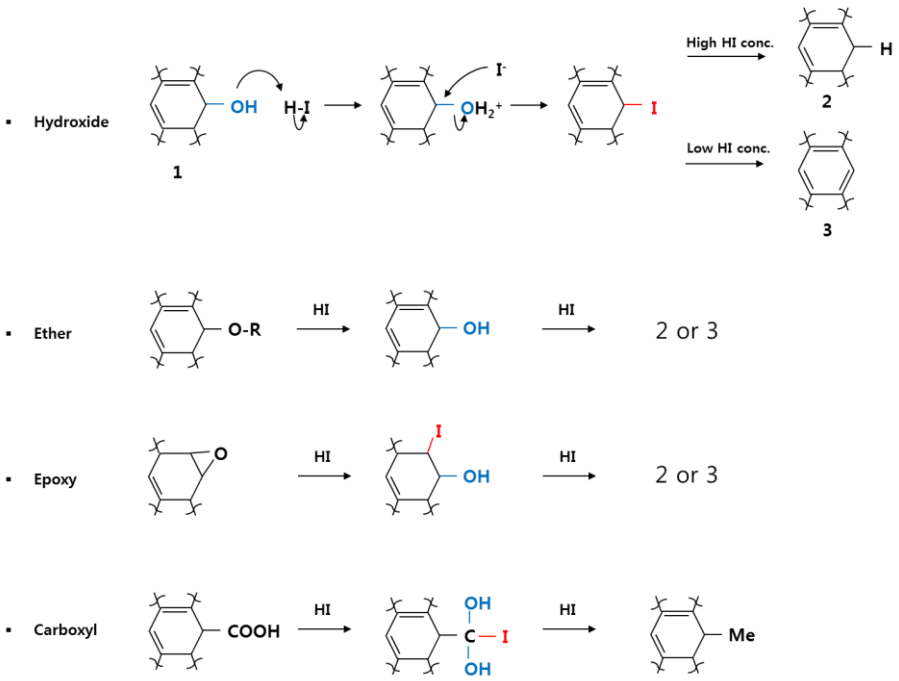

Figure 3. Expected Reduction Mechanism of Hydroiodic Acid

2. Fabrication and Reduction of Graphene Oxide fiber

2.1 Synthesis and characterization of graphene oxide liquid crystals

2.1.1 Graphene oxide liquid crystal synthesis

The graphene oxide liquid crystal solution was prepared by the following method. Natural graphite (10 g) was mixed in a mixed solution of concentrated sulfuric acid (98% sulfuric acid, 150 mL) and concentrated nitric acid (78% fuming nitric acid, 50 mL) for 24 hours. After installing an ice bath, 1.7 L of distilled water was added slowly and diluted and left overnight. After washing to neutralization through vacuum filtration and drying at 60℃ for 24 hours, expandable graphite was obtained. The dried expandable graphite was heat treated in a microwave oven for 5 seconds to obtain expanded graphite. The expanded graphite undergoes pre-oxidation. $K_2S_2O_8$ (potassium persulfate, 2.1 g) and P_2O_5 (phosphorus pentoxide, 3.1 g) were added to sulfuric acid (98%, 200 mL) and heated at 80℃ for 5 hours with expanded graphite (2 g). The solution was cooled, placed in an ice bath, diluted by adding 2 L of distilled water, washed through vacuum filtration, and dried at 60℃ for 12 hours. From the dried samples, graphene oxides were synthesized by the Hummer method. 2 g of computerized graphite was added to concentrated sulfuric acid (98%, 200 mL) and mixed for 24 hours. $KMnO_4$ (potassium permanganate, 15 g) was added, and after mixing for

24 hours, 1.7 L of distilled water was added very slowly in an ice bath. Since the temperature of the solution rapidly increased by distilled water at this time, a very small amount of the solution was added and the temperature of the solution was kept below 20℃. H_2O_2 (28% hydrogen peroxide, 10 mL) was injected at a rate of 400 $\mu L \cdot min^{-1}$ with a syringe pump. 200 mL of HCl was added, and the mixture was allowed to stand overnight. The transparent supernatant and the brown precipitate are separated. After removing the supernatant, only the precipitate is collected and centrifuged to neutralize and concentrate. Neutralization was performed by centrifugation at 15,000 rpm for 10 minutes to remove the supernatant, re-dispersing the supernatant by adding distilled water, and repeating the above procedure five times in total to prepare a neutral solution. The neutralized solution was centrifuged at 3,000 rpm to remove the lowest black impurity. The solution from which impurities were removed was centrifuged at 20,000 rpm to remove the supernatant, and only the precipitate was obtained to prepare a highly concentrated graphene oxide solution.

2.1.2 Characterization of graphene oxide liquid crystals

Cross-polarized optical microscope

For image capturing of Cross-Polarized Optical Microscope (POM), the graphene oxide solution was diluted to 1 mg · mL^{-1} in distilled water. The diluted solution was dispersed for 5, 10, 30, and 60 minutes using an ultrasonicator, and each 1 mL was taken and transferred to a cuvette.

Scanning Electron Microscope

A scanning electron microscope (SEM) image was used to identify the graphene oxide particle distribution. Samples were prepared by the following procedure for SEM image measurement. The silicon wafers were cut into 1×1 cm, cleaned with distilled water and acetone, placed in a plasma cleaner, and plasma-treated at 18 W for 25 seconds while injecting the dried air at 1 torr. The surface treated wafers were placed in a Petri dish and left in a silanization solution for 30 minutes. The silanization solution was prepared so that the volume ratio of APTES (3-aminopropyl trimethoxysilane), acetic acid and methanol was 3: 5: 100, respectively.[40] The solution-treated wafers were taken out, washed in distilled water, and left in a graphene oxide solution diluted to 10 μg · mL^{-1} for 30 minutes. The wafers loaded with graphene oxide on the surface were

lightly washed with running distilled water, and then the surface was photographed on an SEM. The average nominal diameter of graphene oxide was measured using software (ImageJ).

2.2 Graphene fiber fabrication and characterization

2.2.1 Graphene fiber fabrication

Fabrication of graphene oxide liquid crystal fiber

The graphene oxide fibers were fabricated by wet spinning with a petri dish method. A 20 mg · mL^{-1} solution of graphene oxide was prepared, filled into a 10 mL syringe, and mounted on a syringe pump. The nozzle was 24G (inner diameter 0.30 mm). The container of the coagulation solution used was a 9 cm diameter petri dish. Petri dish was installed in the center of the turntable. The syringes and nozzles were oriented perpendicular to the surface of the petri dish, and the tip of the nozzle was bent to level. The tip of the nozzle was oriented 3 cm away from the center of the petri dish so that it was horizontal to the direction of rotation tlzu. A 0.5 mg · mL^{-1} CTAB aqueous solution was used as the coagulation solution. The graphene oxide dope was performed at a speed of 400 μm · min^{-1}, and the rotating plate was rotated at a speed of 30 rpm. The graphene oxide gel fibers were prepared and left in the coagulation solution for 20 minutes. The fibers were taken out and washed out in distilled water, fixed again on both ends, and dried overnight to naturally produce graphene oxide fibers.

Reduction of graphene oxide liquid crystal fiber

To fabricate graphene oxide fibers, graphene oxide fibers were reduced in various concentrations of HI / AcOH solution. HI was added with acetic acid as a solvent at concentrations of 2, 5, 10, 15, 20, 25 and 30 wt%, and then mixed using a vortex mixer. The HI / AcOH solution was used within 10 minutes immediately after preparation. Graphene oxide fibers were added to various concentrations of HI / AcOH and reduced at room temperature for 24 hours. The reduced fiber was placed in a 6% aqueous solution of $NaHCO_3$, and the residual acid was removed from the shaker at 40 rpm for 1 hour. Then, the fiber was transferred to distilled water and washed repeatedly by repeating the same shaking process as above. The washed fibers were taken out, the both ends were fixed and hanged overnight to dry naturally to produce reduced graphene oxide fibers.

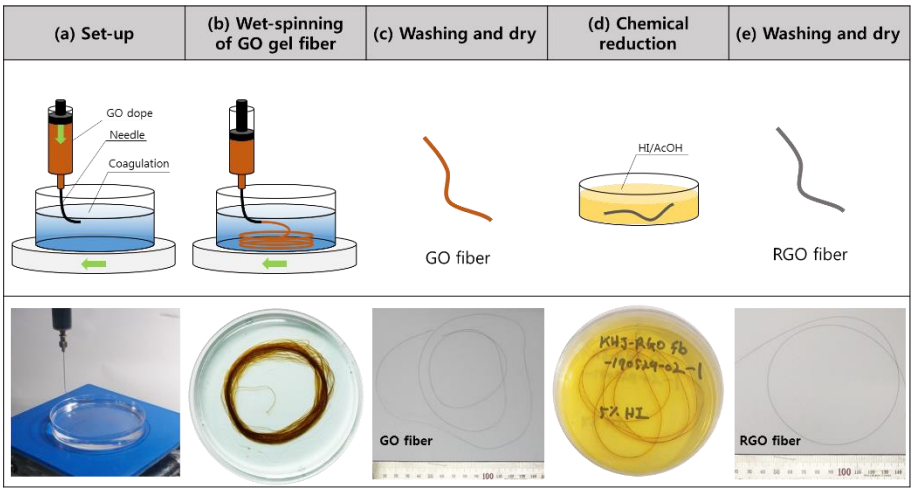

Figure 4. A schematic and actual image of the wet spinning and reduction process

2.2.2 Characterization of graphene fiber

Graphene oxide liquid crystal properties

An electron microscope (SEM) image, a microscope (OM) image and a cross-polarized image were taken to confirm the liquid crystal properties of the graphene oxide solution.

The distribution of graphene oxide particles before and after centrifugation was compared in order to compare the solution characteristics with the influence of impurities and particle size. It was confirmed that the distribution of particles varies greatly depending on the presence or absence of impurity treatment. When the impurity treatment was carried out, it was confirmed that the un-peeled particles were hardly found and the sizes of the particles were relatively uniform. These characteristics strongly influence the dispersion of the solution and the formation of the nematic phase, suggesting that the impurity removal process is essential for securing the liquid crystal solution.

In order to compare the liquid crystal properties according to the size distribution of graphene oxide particles, cross-polarized images were obtained by ultrasonication of graphene oxide solution over time. Ultrasound dispersion physically breaks graphene oxide particles to reduce particle size.[22] Therefore, it is possible to control the grain size of graphene oxide by

controlling the intensity and time of ultrasonic dispersion, and the effect of particle size on the liquid crystal characteristics was confirmed using this. From the control group graphene oxide solution (0 min) dispersed without ultrasonic treatment to the solutions treated with ultrasonic treatment for 5 minutes, 10 minutes, 30 minutes and 60 minutes were respectively prepared and the polarized images were confirmed. As a result, a clear change in the liquid crystal phase was confirmed. As the ultrasonic treatment time increases, the particle diameter decreases from 7.66 μm to 0.89 μm on average, and birefringence phenomenon disappears gradually. The liquid crystal properties, which appear very clearly in the control group, imply a firm nematic phase, while the nematic area decreases as the particle size decreases and eventually becomes isotropic through the dual phase state. This is in agreement with the fact that as the aspect ratio of graphene oxide particles increases, the critical concentration decreases and the nematic phase appears. Based on these results, it can be expected that continuous graphene oxide fiber fabrication is possible when the graphene oxide particles are several micrometers or more.

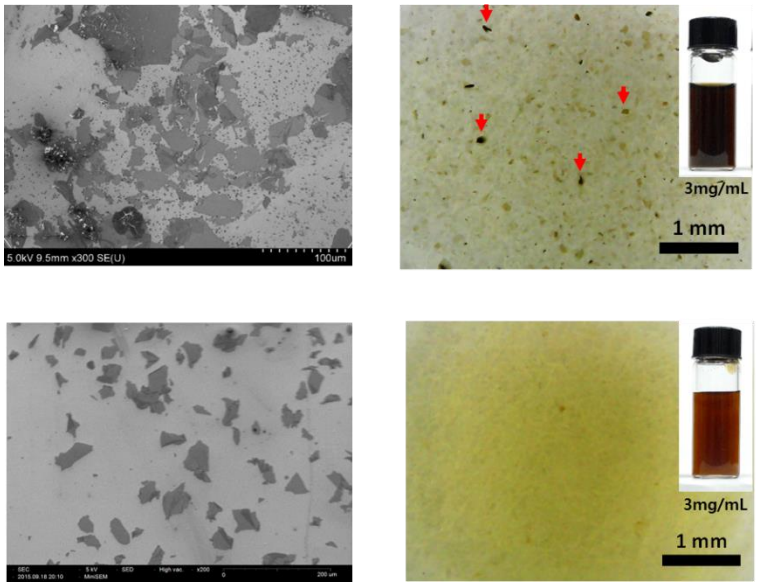

Figure 5. OM images and SEM images of graphene oxide solutions

Cross-polarized image					
Sonication time (min)	0	5	10	30	60
Average size (μm)	7.66	6.19	4.83	2.83	0.89

Figure 6. Average particle size and polarized image of graphene oxide with different ultrasonic treatment time

Size distribution of graphene oxide liquid crystal particle

Nominal mean diameters of particles were calculated from SEM images of graphene oxide solutions sorted by particle size through ultrasonic treatment time. The SEM image shows a clear change in the overall particle size. It can be seen that when the ultrasonic wave is treated for 60 minutes, the average diameter is folded into the nanometer range. From the dispersion of the particle size and the polarization image, we can expect a diameter region that affects the nematic phase. On the polarized image, the liquid crystal properties are greatly changed between the solution treated for 10 minutes with ultrasound and the solution treated for 30 minutes. On the other hand, in the particle distribution graph, the presence of particles in the region of about 50 μm to 100 μm is compared between the two solutions. Based on this, it can be deduced that the nematic–isotropic phase transition seen in the polarized image is caused by the particle size of 50 μm ~ 100 μm.

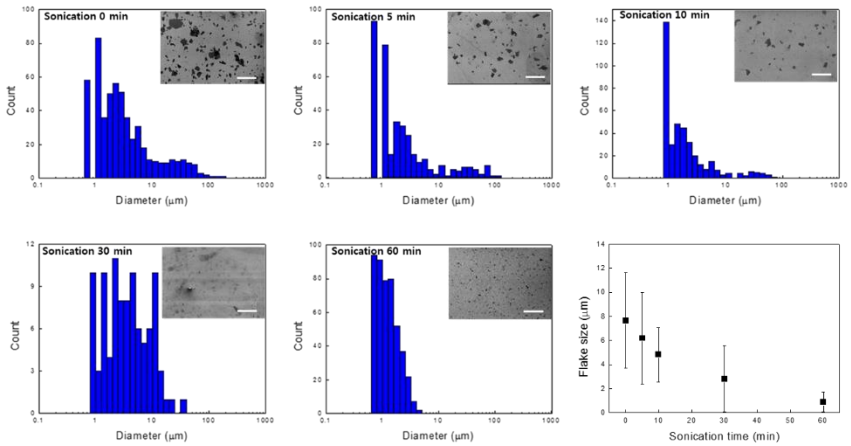

Figure 7. SEM image based graphene oxide particle distribution analysis

Tensile strength

The mechanical strength of the graphene oxide fibers reduced to 5.3% and 28.6% HI / AcOH was measured. The results are 133.5mN · tex^{-1} and 87.9mN · tex^{-1}, respectively. That is, the mechanical strength of the reduced graphene oxide fiber was measured to be high in a low concentration environment. This is expected to be due to the difference in the bond formed due to the different route of the reaction depending on the reduction mechanism of HI. The graphene oxide fibers reduced to a high concentration (28.6%) HI mixture retain sp^3 hybrid orbital even after functional removal. Since the oxygen functional group is removed, the hydrogen bonding ability is lacking. However, since the sp3 bond structure is still maintained, only van der Waals force acts on the reduced graphene layer. On the other hand, the graphene oxide fiber reduced to low concentration (5.3%) HI mixture transforms into sp^2 hybrid orbitals after functional removal and restores double binding ability. Thus, the p orbitals not participating in the hybridization bond are oriented perpendicular to the graphene layer, overlapping between the p-orbits of the layer to form a weak π bond. This means that the molecular structures of the reduced graphene oxide fibers at the low and high concentrations are different, suggesting that the mechanical strength varies due to the difference in structure.[41]

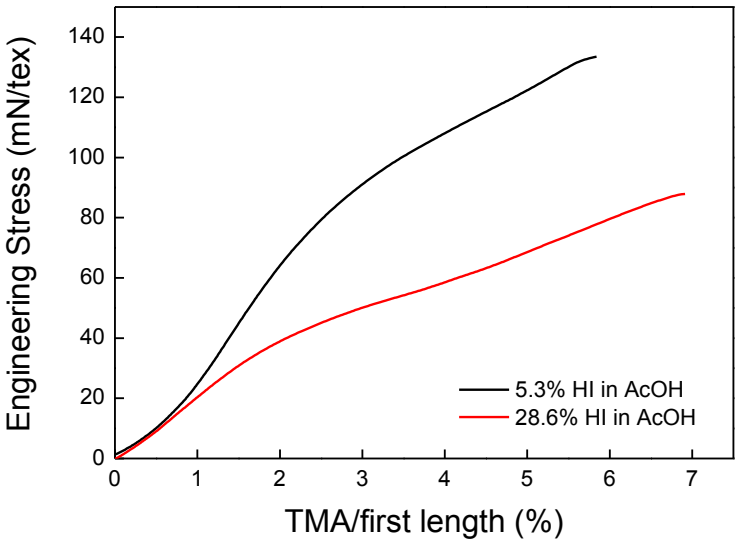

Figure 8. Tensile strength measurement of graphene fibers

Structure analysis

Optical microscopy and scanning electron microscope images were taken to analyze the structure of the reduced graphene oxide fibers. As a result of calculation of the average diameter according to the reducing agent concentration of the graphene fibers, it was confirmed that the thickness of the reduced fiber in the low concentration HI environment was reduced. It was confirmed that the thickness increased about 30% from at least 52 μm (2% HI / AcOH) to 68 μm (25% HI / AcOH). This is expected to be due to a similar cause as the previously measured mechanical strength. The change of HI concentration seems to influence the product reaction path of the graphene structure in the fiber. In the low concentration HI / AcOH region, the p orbitals were oriented perpendicular to the graphene axis through the recovery of double bonds and the formation of sp^2 hybrid orbitals, which causes superposition of $\pi - \pi$ between the layers, so that intergranular bonding becomes stronger. Particularly in this process, the interlayer distance decreases and the thickness of the fiber becomes macroscopically thin.

On the other hand, in the high concentration of HI / AcOH region, the functional group is replaced with hydrogen and the sp^3 hybrid orbital is maintained. Although the repulsive effect due to the oxygen functional groups between the layers existing in the graphene oxide disappears, the attraction effect due to

superposition of the interlayer $\pi-\pi$ is relatively small because sp^2 bonds are smaller than those of the spin wires. Thus, this suggests that fiber thickness increases at the macroscopic point.

The surface and cross-sectional structure of reduced graphene fibers fabricated from 28.6% high-concentration reducing agent were confirmed by scanning electron microscope. On the fiber surface, the grains of the reduced graphene oxide produced by the shrinkage are aligned horizontally on the fiber and are firmly aligned. Particularly, it can be seen that a layered structure is formed and accumulated on a sectional image. This structural feature implies that graphene oxide liquid crystals are effectively aligned to form a nematic phase in the wet spinning process.

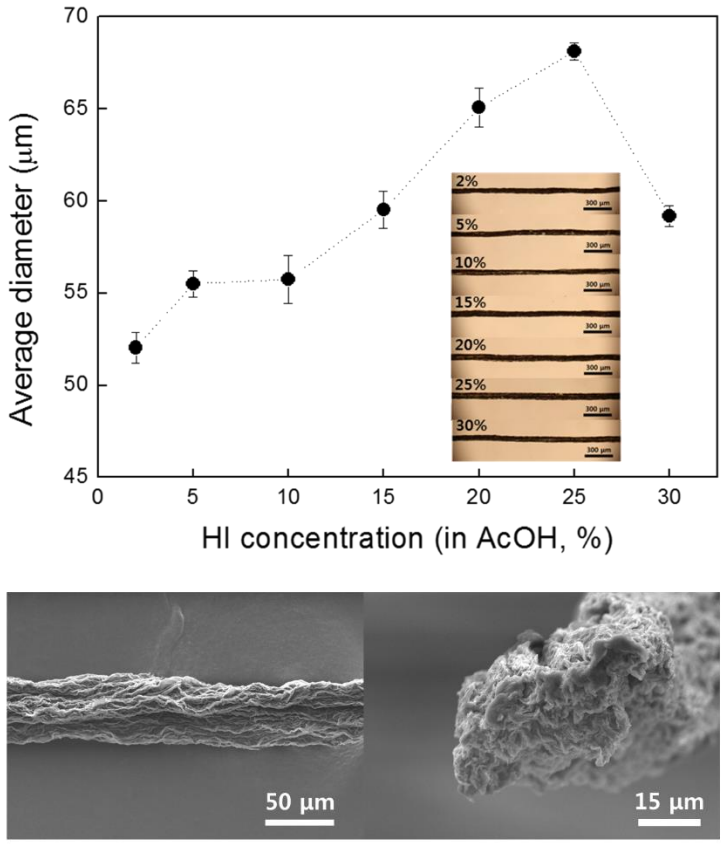

Figure 9. Average diameter of Reduced Graphene Oxide Fibers and Observation of Surface Structure. (Above) OM observation and thickness measurement image of graphene oxide fiber reduced by HI concentration, (below) SEM image of graphene oxide fiber reduced under 28.6% HI / AcOH

Electrical conductivity

Electrical conductivity measurements were made by fixing the graphene oxide fibers on a slide glass, applying silver paste on both ends and measuring the I-V in a two-probe manner.

Conductivity of graphene oxide fibers showed a tendency to change with HI concentration. The highest conductivity (1230 $S \cdot m^{-1}$) was observed under 10% HI / AcOH condition. Conductivity decreased continuously when HI concentration increased beyond 10% HI / AcOH. This is expected to be caused by the fact that the path of the reduction product varies depending on the HI concentration. According to the above-mentioned HI reduction mechanism, sp^3 bond is formed under the high concentration reducing agent condition, sp^2 bond is formed under the low concentration reducing agent condition, and only the latter produces the double bond, thereby recovering the graphene characteristic. The C/O ratios of the individual fibers are similar under the assumption that the reduction has progressed sufficiently regardless of the HI concentration, but the electric conductivity will vary depending on whether a double bond is formed or not. Therefore, it can be assumed that the change in conductivity of the reduced graphene oxide fiber due to the change in HI concentration is a result of the difference in the structure of the product. On the other hand, the result of HI

/ AcOH reduction condition of 5% or less shows a tendency to decrease the conductivity again. This is expected to occur when the reducing agent concentration becomes gradually thinner and the reduction reaction cannot proceed sufficiently. Therefore, it is assumed that the C/O ratio decreases at the concentration. It is also possible to indirectly deduce the double bond recovery state of the reduced graphene oxide fiber through electrical conductivity measurement and to control the electrical characteristics of the graphene oxide fiber by changing the reduction concentration of HI.

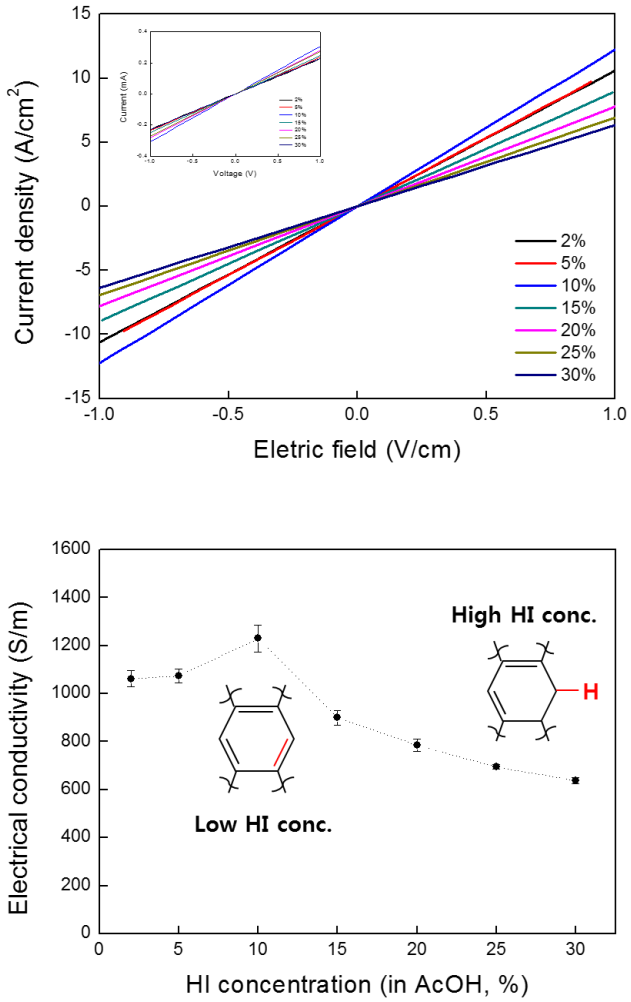

Figure 10. Results of reduced graphene oxide I–V and electrical conductivity measurements with varying HI / AcOH concentrations. (above) The I–V measurement of the reduced graphene oxide fiber, (below) the electrical conductivity of the reduced graphene oxide fiber according to the concentration of the reducing agent

Capactiance analysis

Electrochemical characteristics were measured by three electrode method. Reduced graphene oxide fibers were fixed on the slide glass, and the ends of the fibers were contacted with the copper substrate, and the silver paste was applied to the top of the substrate. The reference electrode was Ag / AgCl and the counter electrode was platinum wire. The electrolyte was a 1M Na_2SO_4 aqueous solution.

The electrochemical characterization of the reduced graphene oxide fibers seems to be affected by the reducing agent concentration. The graphene oxide fibers were reduced in 5.3% and 28.6% HI / AcOH, respectively, to confirm the effect of the product changes mentioned above. For the cyclic voltammetry (CV) measurement, the voltage was applied to the two fibers at a scan rate of 10 mVs^{-1} and showed a specific capacitance (C_{sp}) of 211 Fg^{-1} and 167 Fg^{-1}, respectively. As a result of calculating the energy density (E_{sp}) and the power density (P_{sp}) from this, the fiber treated with 5.3% HI / AcOH exhibited a maximum energy density of 29.3 $Wh \cdot kg^{-1}$ (10 mVs^{-1}) and a maximum power density of 7018 Wkg^{-1} (1 Vs^{-1}). The fibers treated with the high-concentration reducing agent exhibited a maximum energy density of 23.2 $Wh \cdot kg^{-1}$ (10 mVs^{-1}) and a maximum power density of 3955 Wkg^{-1} (1 Vs^{-1}). In all respects, the performance of low-concentration reduced graphene oxide

fibers precedes. On the CV graph, 5.3% HI / AcOH reduced fibers are found to charge much more rapidly in the initial 0−0.2V section. This has a similar meaning to the previously measured I−V results. It is believed that the electrical conductivity increases due to the double bonds recovered in the low concentration reduction process, which is supported by the high power density results. Conversely, 28.3% HI / AcOH reduced graphene oxide fibers exhibit a mild CV charge / discharge pattern due to their low power density. Compared with low density reduced fibers, the energy density is about 80%, but the output density is about 56%. The difference in the performance of the two graphene oxide fibers seems to be mainly due to the internal resistance, suggesting that the characteristics have greatly changed from whether or not the double bond is recovered after reduction.

The energy storage characteristics of the two fibers were calculated by the following equation.

$$C_{sp} = \frac{\int I dV}{M \times \Delta V \times S} \quad \text{(Equation 6)}$$

$$E_{sp} = \frac{1}{2} C_{sp} V^2 \quad \text{(Equation 7)}$$

$$P_{sp} = \frac{E_{sp}}{\Delta t} \quad \text{(Equation 8)}$$

Where I is the measured current, V is the applied voltage, M is the mass of the electrode material S is the scanning speed, and ⊿t is the time taken for the discharge.

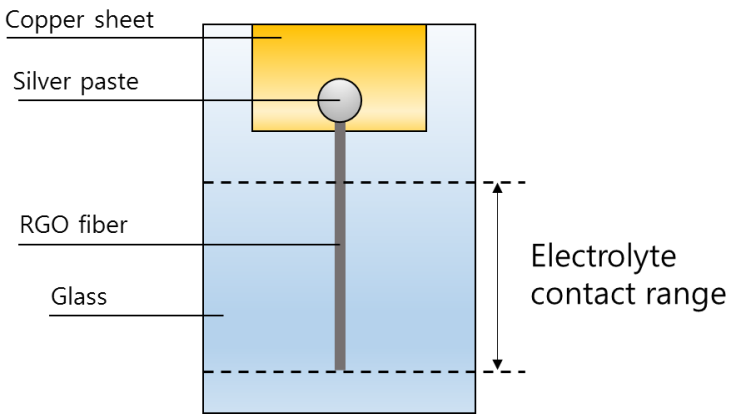

Figure 11. A schematic diagram of a cell for reduced graphene oxide fiber electrochemical measurements

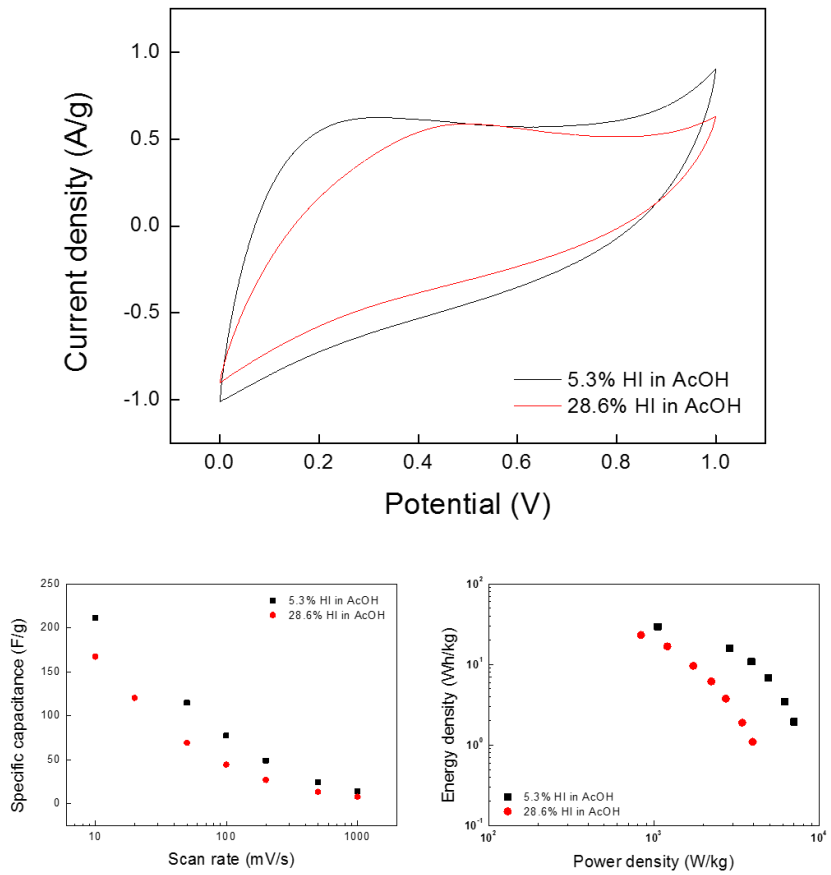

Figure 12. Electrochemical properties of reduced graphene oxide fibers with HI / AcOH concentration

3. CuI-RGO fiber fabrication and sensor research

In this study, reduced graphene oxide (CRGO) fibers with copper iodide (CuI) and copper (Cu) particles were fabricated and the characteristics of multi-sensor were verified. This fiber was prepared by the simultaneous preparation of Cu particles and RGO by inserting and reducing precursor ions of Cu particles into graphene oxide (GO) during wet spinning process. Copper ion (Cu_2^+) was added to ethyleneglycol (EG) and used as a coagulation solution. The GO dope was injected to produce fibers by wet spinning. The GO composite fiber contained a large amount of copper oxide (CuO) particles. It was confirmed that the reduced CRGO fibers reduced using hydroiodic acid (HI) contained CuI and Cu particles. The fabricated CRGO fiber contains a large amount of Cu ions and has a dense and wrinkled structure including rich pores. It was confirmed that the insertion of CuI and Cu particles can control the humidity dependence, crystallinity and porosity of the electrical properties of graphene oxide. Especially, CRGO showed different gas detection ability and temperature detection ability depending on Cu concentration.

Chlorobenzene is a raw material used in various industries, and is used in large quantities for dyes, paints and insecticides (DDT). But it is classified as a Class 4 dangerous substance in Korea. Inhalation of vapors causes central nervous system paralysis and

deposits in body fat during long-term exposure, resulting in neurological symptoms such as sensory paralysis or hypersensitivity, cyanosis, and muscle stiffness.[47] It is a substance that is used extensively in daily life and therefore requires accurate and rapid detection. It was found that the CRGO fiber showed a larger current change when exposed to chlorobenzene at higher Cu contents. CRGO fiber containing 10% of Cu (CRGO-10) exhibited the largest current change (~ 6.5 μA) according to chlorobenzene exposure, and the current change recovered to its initial state when the gas exposure was stopped. The change in the conductivity of the CRGO fiber depends on the amount of chemisorbed gas adhere on the metal oxide surface.

On the other hand, CRGO fibers showed the ability to detect the temperature change, which showed a high current change in the fibers with low Cu content ratio as opposed to the gas sensing ability. In particular, the CRGO fiber with 1% Cu content (CRGO-1) showed the largest current change (~13 μA) even at low temperature increase (5℃) . Since the resistance change of Cu according to temperature is relatively small compared to the resistance change of GO, CRGO fiber containing less Cu is advantageous for temperature detection.

Based on these results, we proposed a twisted-pair multi-detector element for two fibers with different Cu content

(CRGO-1, CRGO-10). The non-conductive polymer was coated on the surface of CRGO-1 to prevent shorting between two fibers. The fabricated sensor is expected to be capable of measuring temperature changes near room temperature and changes in gas (chlorobenzene) concentration in air in real time.

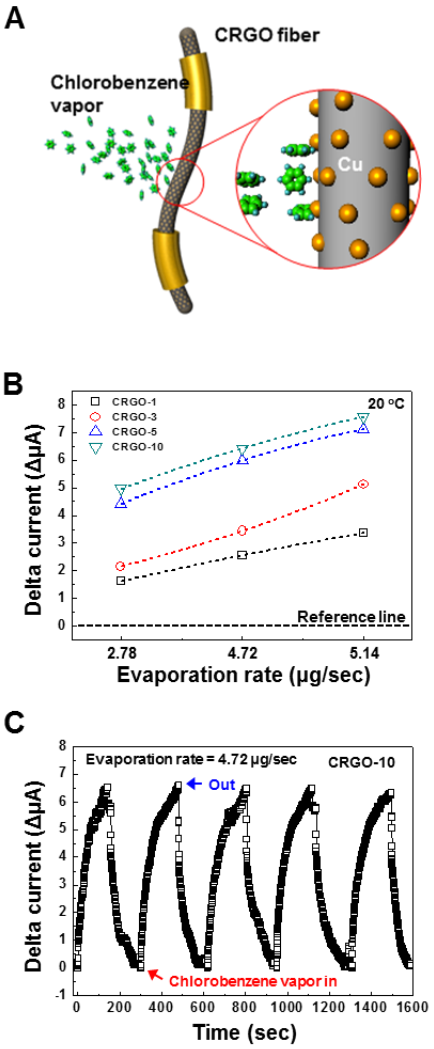

Figure 13. Detection Characteristics of Chlorobenzene in CRGO Fiber. (A) A schematic diagram of the chlorobenzene detection process of CRGO fibers. (B) Chlorobenzene detection characteristics according to Cu concentration change of CRGO. (C) Chlorobenzene detection on-off characteristic of CRGO-10.

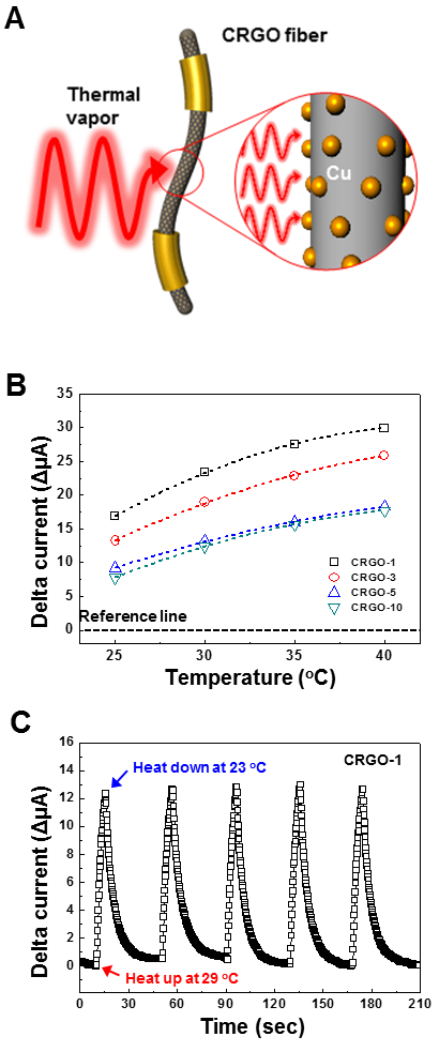

Figure 14. Detection Characteristics of Temperature Change of CRGO Fiber. (A) A schematic diagram of the process of detecting temperature change of CRGO fiber. (B) Temperature Change Detection Characteristics of CRGO with Variation of Cu Concentration. (C) Temperature change detection on-off characteristic of CRGO-1.

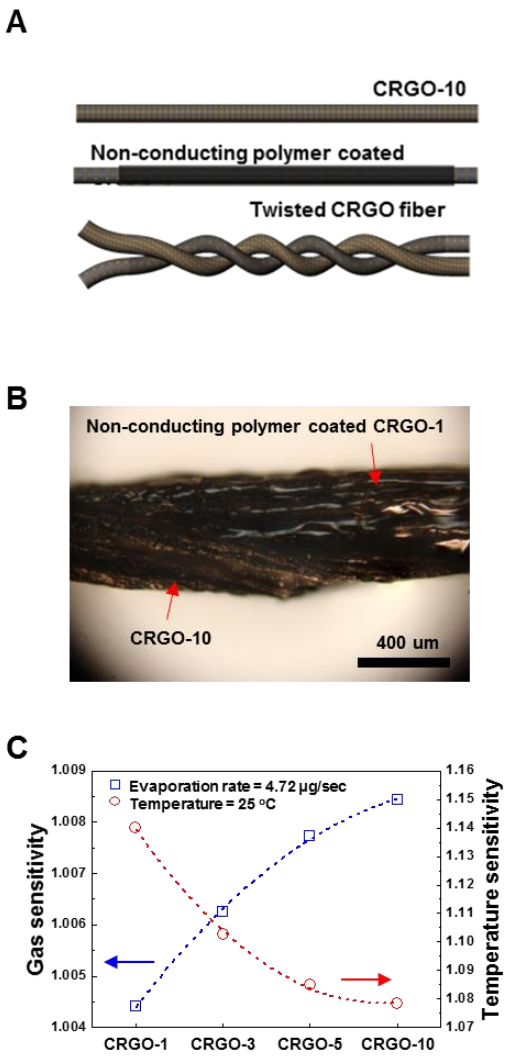

Figure 15. CuI−RGO composite fibers for multiple detection. (G, H) Sensor configuration diagram and image of two CRGO fibers with different detection characteristics. (I) Multiple Detection Characteristics of CRGO.

4. All-graphene supercapacitor research

In this study, we fabricated graphene oxide (GO) and reduced graphene oxide (RGO) film-based supercapacitors and maximized energy storage characteristics through acid-thermal treatment process. Also, we confirmed that pulse energy of 20 ms is stored, and suggested the possibility of interworking with energy harvesting device.

The graphene oxide-based supercapacitor (AGO supercapacitor), which was fabricated using RGO film as the active electrode and GO film as the separator, was heated at 80~84℃ with 4M sulfuric acid aqueous solution. Through this process, the sulfuric acid molecules penetrate deeply into the RGO and GO film, which is confirmed by the reduction of the sulfuric acid peak intensity before and after the heat process on the Raman spectroscopic measurement results. Thus, the GO film with sulfuric acid can simultaneously serve as a quasi-solid-state liquid electrolyte and a separator. The acid-thermal treated supercapacitor at 84℃ showed an energy storage capacity of 125.6 Fcm^{-3} at a scanning speed of 100 mVs^{-1} as measured by the cyclic voltammetry (CV) method, which is 93.7 times higher value than that of the device not acid-thermal-treated. In addition, when acid-thermal-treated at 84℃, the capacitance at a scanning speed of 10 mVs^{-1} was 266 Fcm^{-3} at

maximum. This phenomenon of increase in energy storage capacity starts to increase sharply from the acid-thermal treatment temperature of 70℃, and the energy storage mechanism is expected to be changed at a temperature of 80℃ or higher. In the acid-thermal treatment process below 80℃, the CV opening is generally in the form of EDLC (Electric Double Layer Capacitor), while in the process above 80℃, the shape of the pseudocapacitive by ion adsorption and surface redox reaction respectively. Above 90℃, the vaporization of water accelerates and the performance decreases.

As a result of SEM measurement, a large surface change was found before and after the acid-thermal treatment. When subjected to acid-thermal treatment, the RGO particles formed a series of particles (RGO islands), which apparently increased the specific surface area. The particles were uniformly distributed within several micrometers. This is very similar to the steam activation process used for porous activated carbon and is expected to form this structure in the course of the mixed steam of sulfuric acid and water.

As a result of applying a pulse voltage of 20 ms to the graphene oxide film-based supercapacitor, it was confirmed that the instantaneous energy can be stored. A basic symmetric SINC (sinus cardinalis) pulse and an ECG (electrocardiogram) pulse similar to a heartbeat were applied to the supercapacitor using a

function generator. As a result, the phenomenon of storing the generated pulses to 1V was observed. Especially, it has been confirmed that supercapacitor can store 1V potential within 200 seconds from ECG pulse, suggesting possibility of interworking with energy harvesting device which is actively studied at present.

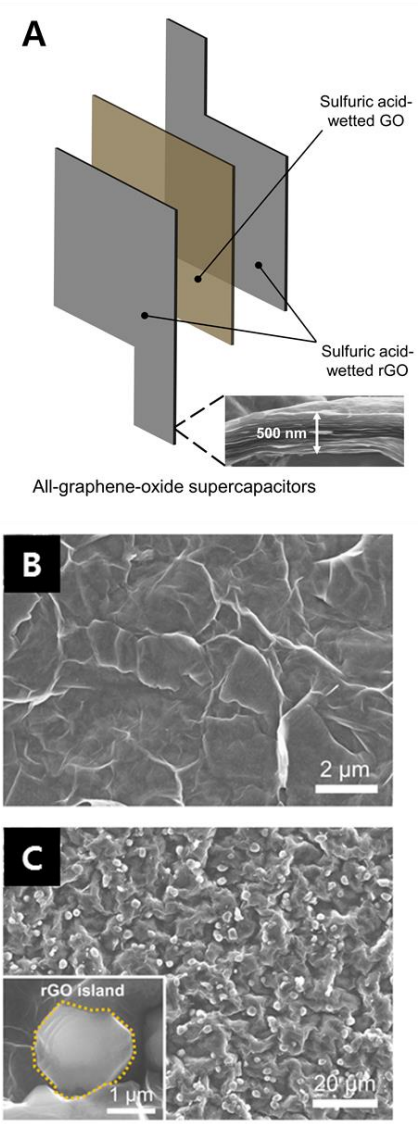

Figure 16. Graphene oxide film based super capacitor. (A) Configuration diagram of AGO supercapacitor. (B) SEM image of sulfuric acid-heat treated GO film. (C) SEM image of sulfuric acid-thermal treated RGO film.

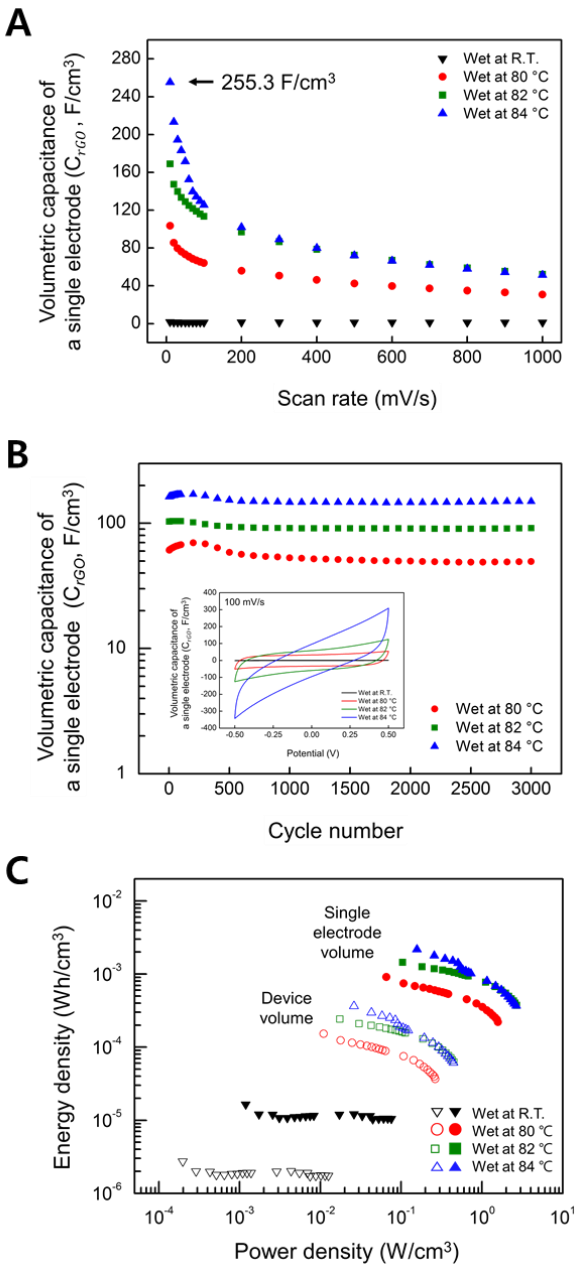

Figure 17. Electrochemical Properties of AGO Super Capacitors.

(A) Comparison of capacitance change with thermal treatment.

(B) Stability test. (C) Ragon chart.

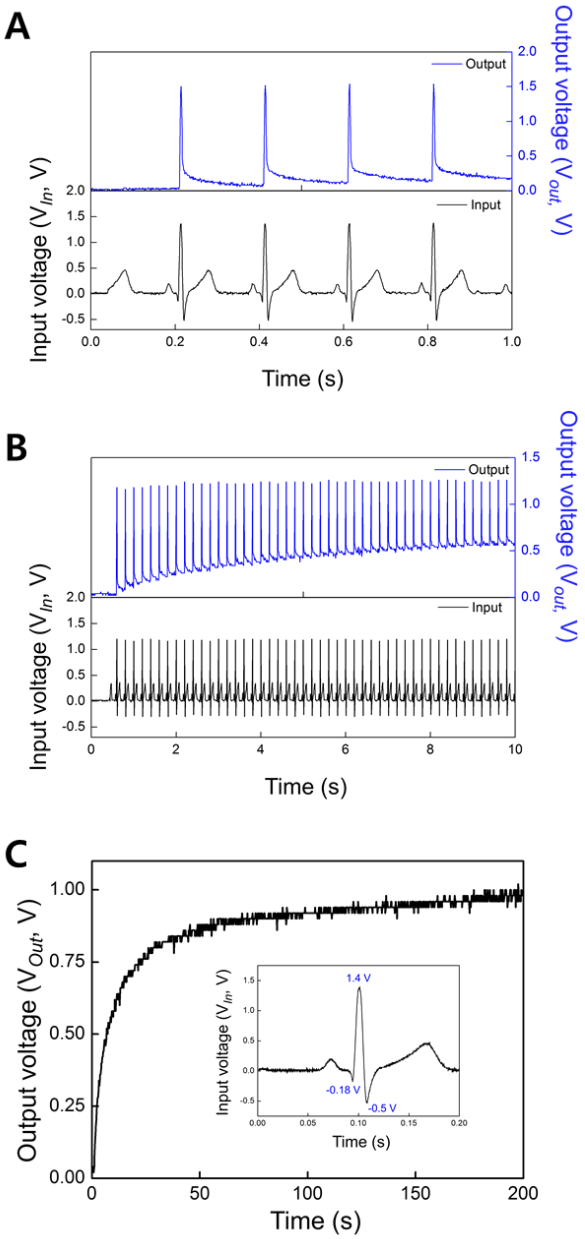

Figure 18. Charge characteristics of AGO supercapacitor measured with 20ms ECG pulse.

5. Conclusion

In this study, we investigated the characteristics of graphene oxide liquid crystals and analyzed the characteristics of graphene oxide fibers according to the reduction mechanism. After the preparation of graphene oxide liquid crystal, particle size was classified according to ultrasonic time and liquid crystal properties were compared. As a result of comparing the liquid crystal characteristics through the cross-polarized image and the average diameter dispersion, it was confirmed that the particles in the range of 50-100 μm had a great influence on the isotropic-nematic phase transition. Graphene oxide fibers were fabricated by wet spinning using graphene oxide liquid crystal, and the characteristics of the fibers were compared and analyzed according to the change of HI / AcOH reducing agent concentration. As a result of measuring the mechanical strength, the tensile strength (133.5 $mN \cdot tex^{-1}$) of the reduced fiber in the low concentration (5.3% HI / AcOH) was higher than the tensile strength (87.0 $mN \cdot tex^{-1}$) of the high concentration reduced fiber (28.6% HI / AcOH). This seems to be related to the reduction of the diameter of the reduced fibers in the low concentration environment (minimum 52 μm maximum 68 μm, 2% and 25% HI / AcOH reduction, respectively). It is suggested that a strong bond is formed by the overlapping of $\pi - \pi$ orbital

formed between the particle layers, reducing the interlayer distance, and the density of the macroscopic fiber becomes thinner at the same time. It is expected that the mechanical strength of fibers with increased density increases with the change of physical properties. As a result of the electroconductivity measurement, the conductivity of the reduced graphene oxide fiber in the 10% HI / AcOH environment was the highest (1230 Sm^{-1}). It seems that the reduction reaction did not occur sufficiently at the low concentration (2~5%), so the conductivity decreases. On the other hand, it seems that hydrogen substitution instead of double bond did not contribute to the increase of conductivity at the higher concentration environment (15~30%). This is related to the decrease in the energy storage capacity as the concentration of the reducing agent used in the electrochemical measurement results decreases. CV morphology of the graphene oxide fibers reduced in the low concentration (5.3%) HI / AcOH exhibited greater energy storage characteristics (211 Fg^{-1} and 167 Fg^{-1}, respectively) than the high concentration (28.6%) reduced sample. This affected the charging rate in the CV opening with changes in electrical conductivity, resulting in a large difference in output density (7018 $W \cdot kg^{-1}$, 3955 $W \cdot kg^{-1}$, respectively).

From these results, it can be concluded that the reduction of graphene oxide by HI / AcOH reducing agent forms a product

with a completely different mechanism pathway depending on the concentration. This has a large influence on the physical, electrical and electrochemical of the reduced graphene oxide fibers. Fundamentally, in order to maximize the properties of the graphene oxide liquid crystal fiber, it is essential to maintain micro-sized particles and uniform the distribution to secure liquid crystal properties. By optimizing the reducing agent condition through the understanding of the reduction mechanism, it is possible to maximize the electrical and electrochemical characteristics of the reduced graphene oxide liquid crystal fiber. Understanding the liquid crystal properties of graphene oxide and optimizing the reduction conditions can realize process completion and texturing of graphene fibers, which will be a cornerstone for the commercialization of wearable flexible devices.

Reference

1. Dr. Wei Weng, Peining Chen, Sisi He, Xuemei Sun, Huisheng Peng, Smart Electronic Textiles, Angew.Chem., (2016) 55, 6140 -6169.

2. Compton OC1, Nguyen ST., Graphene oxide, highly reduced graphene oxide, and graphene: versatile building blocks for carbon-based materials, Small (2010) 6, 711-723.

3. Haiyan Sun, Zhen Xu, Chao Gao, Multifunctional, Ultra-Flyweight, Synergistically Assembled Carbon Aerogels, Adv. Mater. (2013) 25, 2554-2560.

4. Yi Han, Zhen Xu, Chao Gao, Ultrathin Graphene Nanofiltration Membrane for Water Purification, Adv. Funct. Mater. (2013) 23, 3693-3700.

5. Yanwu Zhu, Shanthi Murali, Weiwei Cai, Xuesong Li, Ji Won Suk, Jeffrey R. Potts, Rodney S. Ruoff, Graphene and Graphene Oxide: Synthesis, Properties, and Applications, Adv. Mater. (2010) 22, 3906-3924.

6. Siegfried Eigler, Michael Enzelberger-Heim, Stefan Grimm, Philipp Hofmann, Wolfgang Kroener, Andreas Geworski, Christoph Dotzer, Michael Röckert, Jie Xiao, Christian Papp, Ole Lytken, Hans-Peter Steinrück, Paul Müller, Andreas Hirsch, Wet Chemical Synthesis of Graphene, Adv. Mater. (2013) 25, 3583-3587.

7. Yi Zhang, Luyao Zhang, and Chongwu Zhou, Review of Chemical Vapor Deposition of Graphene and Related Applications, Acc. Chem. Res., (2013) 46 (10), 2329-2339.

8. Cecilia Mattevi, Hokwon Kima, Manish Chhowalla, A review of chemical vapour deposition of graphene on copper, J. Mater. Chem., (2011) 21, 3324-3334.

9. William S. HummersJr., Richard E. Offeman, J. Am. Chem. Soc., (1958) 80 (6), 1339-1339.

10. Tian-Zi Shen, Seung-Ho Hong, Jang-Kun Song, Electro-optical switching of graphene oxide liquid crystals with an extremely large Kerr coefficient, Nature Materials (2014) 13, 394-399.

11. Zhen Xu, Chao Gao, Graphene in Macroscopic Order: Liquid Crystals and Wet-Spun 섬유s, Acc. Chem. Res., (2014) 47 (4), 1267-1276.

12. Cécile Zakri, Christophe Blanc, Eric Grelet, Camilo Zamora-Ledezma, Nicolas Puech, Eric Anglaret, Philippe Poulin, Research article: Liquid crystals of carbon nanotubes and graphene, Phil. Trans. R. Soc. A (2012) 371, 20120499.

13. Zhen Xu and Chao Gao, Aqueous Liquid Crystals of Graphene Oxide, ACS Nano, (2011) 5 (4), 2908-2915.

14. Rouhollah Jalili, Seyed Hamed Aboutalebi, Dorna Esrafilzadeh, Roderick L. Shepherd, Jun Chen, Sima Aminorroaya-Yamini, Konstantin Konstantinov, Andrew I. Minett, Joselito M. Razal, Gordon G. Wallace, Scalable One-Step Wet-Spinning of Graphene fibers and Yarns from Liquid Crystalline Dispersions of Graphene Oxide: Towards Multifunctional Textiles, Adv. Funct. Mater. (2013) 23, 5345-5354.

15. Xueyan Zhu, Quanzi Yuan, Ya-Pu Zhao, Phase transitions of a water overlayer on charged graphene: from electromelting to electrofreezing, Nanoscale, (2014) 6, 5432-5437.

16. Andriy V. Kityk, Mark Busch, Daniel Rau, Sylwia Calus, Carole V. Cerclier, Ronan Lefort, Denis Morineau, Eric Grelet, Christina Krause, Andreas Schönhals, Bernhard Frickg, Patrick Huber, Thermotropic orientational order of discotic liquid crystals in nanochannels: an optical polarimetry study and a Landau-de Gennes analysis, Soft Matter, (2014) 10, 4522-4534.

17. Keith E. Whitener Jr., Paul E. Sheehan, Graphene synthesis, Diamond & Related Materials, (2014) 46, 25-34.

18. Tapas Kuila, Ananta Kumar Mishra, Partha Khanra, Nam Hoon Kim, Joong Hee Lee, Recent advances in the efficient reduction of graphene oxide and its application as energy storage electrode materials, Nanoscale, (2013) 5, 52-71.

19. Mi Se Chang, Yern Seung Kim, Jong Hun Kang, Jisoo Park, Sae Jin Sung, Soon Hyeong So, Kyung Tae Park, Seung Jae Yang, Taehoon Kim, Chong Rae Park, Guidelines for Tailored Chemical Functionalization of Graphene, Chem. Mater. (2017) 29, 307−318.

20. Zhen Xu, Haiyan Sun, Xiaoli Zhao, Chao Gao, Ultrastrong 섬유s Assembled from Giant Graphene Oxide Sheets, Adv. Mater. (2013) 25, 188-193.

21. Songfeng Pei, Jinping Zhao, Jinhong Du, Wencai Ren, Hui−Ming Cheng, Direct reduction of graphene oxide films into highly conductive and flexible graphene films by hydrohalic acids, CARBON (2010) 48, 4466-4474.

22. Chujiang Cai, Nannan Sang, Zhigang Shen, Xiaohu Zhao, Facile and size−controllable preparation of graphene oxide nanosheets using high shear method and ultrasonic method, Mater. Sci. (2014) 49, 1785.

23. Shibing Ye, Jiachun Fen, The effect of sonication treatment of

graphene oxide on the mechanical properties of the assembled films, RSC Adv., (2016) 6, 39681-39687.

24. Ece Özçakir, Büşra Balli, Volkan Eskizeybek, Fabrication of Macroscale Graphene 섬유s via Wet Spinning, IC2NAM, (2016) May 20.

25. Huai-Ping Cong, Xiao-Chen Ren, Ping Wang, Shu-Hong Yu, Wet-spinning assembly of continuous, neat, and macroscopic graphene fibers, Scientific Reports, (2012) 2, 613.

26. Fancheng Meng, Weibang Lu, Qingwen Li, Joon-Hyung Byun, Youngseok Oh, Tsu-Wei Chou, Graphene-Based Fibers: A Review, Adv. Mat. (2015) 27, (35) 5113-5131

27. Ji Eun Kim, Tae Hee Han, Sun Hwa Lee, Ju Young Kim, Chi Won Ahn, Je Moon Yun, Sang Ouk Kim, Graphene Oxide Liquid Crystals, Angew. Chem., (2011) 50, 3043 -3047.

28. Chun Hung Lui, Li Liu, Kin Fai Mak, George W. Flynn, Tony F. Heinz, Ultraflat graphene, Nature (2009) 462, 339-341.

29. Viet Hung Pham, Tran Viet Cuong, Seung Hyun Hur, Eunsuok Oh, Eui Jung Kim, Eun Woo Shin, Jin Suk Chung, Chemical functionalization of graphene sheets by solvothermal reduction of a graphene oxide suspension in N-methyl-2-pyrrolidone, J. Mater. Chem., (2011) 21, 3371-3377.

30. Peng-Gang Ren, Ding-Xiang Yan, Xu Ji, Tao Chen, Zhong-Ming Li, Temperature dependence of graphene oxide reduced by hydrazine hydrate, Nanotechnology, (2011) 22, 055705.

31. Ok-Kyung Park, Myung Gwan Hahm, Sungho Lee, Han-Ik Joh, Seok-In Na, Robert Vajtai, Joong Hee Lee, Bon-Cheol Ku, Pulickel M. Ajayan, In Situ Synthesis of Thermochemically Reduced Graphene

Oxide Conducting Nanocomposites, Nano Lett., (2012) 12, 1789-1793.

32. Hannes C. Schniepp, Je-Luen Li, Michael J. McAllister, Hiroaki Sai, Margarita Herrera-Alonso, Douglas H. Adamson, Robert K. Prud'homme, Roberto Car, Dudley A. Saville, Ilhan A. Aksay, Functionalized Single Graphene Sheets Derived from Splitting Graphite Oxide, J. Phys. Chem. B, (2006) 110 (17), 8535-8539.

33. Cecilia Mattevi, Goki Eda, Stefano Agnoli, Steve Miller, K. Andre Mkhoyan, Ozgur Celik, Daniel Mastrogiovanni, Gaetano Granozzi, Eric Garfunkel, Manish Chhowalla, Evolution of Electrical, Chemical, and Structural Properties of Transparent and Conducting Chemically Derived Graphene Thin Films, Adv Funct Mater (2009) 19, (16) 2577-2583.

34. Xuan Wang, Linjie Zhi, Klaus Müllen, Transparent, Conductive Graphene Electrodes for Dye-Sensitized Solar Cells, Nano Lett., (2008) 8, (1) 323-327.

35. Wei Gao, Lawrence B. Alemany, Lijie Ci, Pulickel M. Ajayan, New insights into the structure and reduction of graphite oxide, Nat. Chem., (2009) 1, 403-408.

36. Hyeon-Jin Shin, Ki Kang Kim, Anass Benayad, Seon-Mi Yoon, Hyeon Ki Park, In-Sun Jung, Mei Hua Jin, Hae-Kyung Jeong, Jong Min Kim, Jae-Young Choi, Young Hee Lee, Efficient Reduction of Graphite Oxide by Sodium Borohydride and Its Effect on Electrical Conductance, Adv. Funct. Mater., (2009) 19, 1987-1992.

37. Jiali Zhang, Haijun Yang, Guangxia Shen, Ping Cheng, Jingyan Zhang, Shouwu Guo, Reduction of graphene oxide via L-ascorbic acid, Chem. Commun., (2010) 46, 1112-1114.

38. Sasha Stankovich, Dmitriy A. Dikin, Richard D. Piner, Kevin A.

Kohlhaas, Alfred Kleinhammes, Yuanyuan Jia, Yue Wu, SonBinh T. Nguyen, Rodney S. Ruoff, Synthesis of graphene-based nanosheets via chemical reduction of exfoliated graphite oxide, Carbon, (2007) 45, 1558-1565.

39. In Kyu Moon, Junghyun Lee, Rodney S. Ruoff, Hyoyoung Lee, Reduced graphene oxide by chemical graphitization, Nat. Commun., (2010) 1, 73.

40. Stanley D. Chandradoss, Anna C. Haagsma, Young Kwang Lee, Jae-Ho Hwang, Jwa-Min Nam, Chirlmin Joo, Surface Passivation for Single-molecule Protein Studies, J. Vis. Exp. (2014) 86, 50549.

41. Zhen Xu, Chao Gao, Graphene chiral liquid crystals and macroscopic assembled fibres, Nat. Commun., (2011) 2, 571

42. Yongchao Si, Edward T. Samulski, Synthesis of Water Soluble Graphene, Nano Lett., (2008) 8 (6), 1679-1682.

43. C. Xiang, C. C. Young, X. Wang, Z. Yan, C.-C. Hwang, G. Cerioti, J. Lin, J. Kono , M. Pasquali, J. M. Tour, Large flake graphene oxide fibers with unconventional 100% knot efficiency and highly aligned small flake graphene oxide fibers, Adv. Mater. (2013) 25, 4592-4597.

44. C. Xiang, N. Behabtu, Y. Liu, H. G. Chae, C. C. Young, B. Genorio, D. E. Tsentalovich, C. Zhang, D. V. Kosynkin, J. R. Lomeda, C.-C. Hwang, S. Kumar, M. Pasquali, J. M. Tour, Graphene Nanoribbons as an Advanced Precursor for Making Carbon Fiber, ACS Nano, (2013) 7, 1628.

45. Daniela C. Marcano, Dmitry V. Kosynkin, Jacob M. Berlin, Alexander Sinitskii, Zhengzong Sun, Alexander Slesarev, Lawrence B. Alemany, Wei Lu and James M. Tour, Improved Synthesis of Graphene Oxide, ACS Nano, (2010) 4 (8), 4806-4814.

46. Hyuk Joon Kim, b, Seul-Yi Lee, Le Hoang Sinh, Chang Su Yeo, Yeong Rae Son, Kang Rae Cho, YoonKyu Song, Sanghyun Ju, Min Kyoon Shin, Soo-Jin Park, SangYoon Park, Maximizing volumetric energy density of all-graphene-oxidesupercapacitors and their potential applications for energy harvest, Journal of Power Sources, (2017) 346, 113-119.

47. R.S.Nair, J.A.Barter, I.R.E.Schroeder, SA.Knezevich, Sandc.R.Stack, Fundamental and applied toxicology, (1987) 9, 678-686

초 록

다기능성 그래핀 액정 섬유제조 및 섬유소자 연구

김 혁 준

나노융합전공

융합과학기술대학원

서울대학교

최근 휴대용 전자장치의 성능이 향상되고 더 많은 기능을 요구함에 따라 전기에너지 저장기술과 유연성 전자소재의 개발이 매우 중요해지면서 인체공학적인 착용형 전자장치 (wearable electronics/devices) 의 제조를 위한 스마트 직물 (smart textile)이 회자되고 있다. 이로 인해 다기능성 신소재에 관한 연구가 각광받고 있으며, 특히 그래핀은 물리적, 전기적 특성으로 인해 귀추를 받고 있다.

그래핀 산화물은 판상형 입자로 인해 액정특성을 보이며, 임계농도 이상에서 isotropic-nematic 상전이를 일으켜 배향성을

갖는다. 이런 특성을 이용해 습식방사를 통한 그래핀 산화물 섬유를 제작이 가능해졌다. 그래핀의 섬유화 기술은 기존의 2D 소재인 필름형 유연성 소자로는 불가능 했던 1D 형태의 직물화 특성을 갖게 되었다. 이러한 그래핀의 섬유화는 매듭짓기, 꼬아 비틀기, 직조 (weaving), 바느질 등이 가능해지면서 웨어러블 소재 및 소자에 특화되고 있다.

본 연구에서는 그래핀 산화물의 액정 특성을 구현하여 특성을 확인하였고, 그래핀 산화물 섬유의 환원 메커니즘에 따른 특성 변화를 연구하였다. 그래핀 산화물 입자 크기에 따른 교차편광 이미지 및 직경 분산도 분석을 통해 그래핀 산화물 액정의 isotropic−nematic 상전이 구간을 확인하였고, 특히 50−100 μm 영역의 입자가 nematic 상에 큰 영향을 주는 사실을 확인하였다. 그래핀 산화물 액정을 사용하여 습식방사를 통해 그래핀 산화물 섬유를 제작한 뒤, HI/AcOH 환원제의 농도의 변화에 따라 환원하여 섬유의 전기전도도 특성을 비교, 분석하였다. 환원제 농도 감소에 따른 섬유 직경 감소 현상으로부터 밀도 증가를 유추하였고, 이는 기계적 강도의 증가로 이어짐을 확인하였다. 전기전도도도 측정에서는 저농도 (10% HI/AcOH) 환원된 섬유의 전기전도도가 고농도 (30% HI/AcOH) 환원된 섬유보다 약 2 배 높게 나타났는데, 이로부터 저농도 환경의 환원이 고농도 환경보다 그래핀 특성을 효과적으로 회복시켰음을 확인하였다. 특히 전하저장 특성 분석에서는 저농도 환원된 섬유가 고농도에 비해 높은 에너지 저장특성(각각 211Fg^{-1}, 167Fg^{-1})을 보였으며, 출력밀도는 약 77% 높게 나타났다. 이와 같은 사실들은 HI 의 농도 조건에 따라 환원 생성물의 경로가 달라지며, 환원 생성물은 이중결합 회복 유무에 따라 환원된 그래핀 산화물 섬유의 특성에 크게 영향을 줄 수 있음을 암시한다.

이러한 결과들로부터 그래핀 산화물 액정 특성 확보 및 환원제 환원 조건 확립을 통해 그래핀 산화물 섬유의 최적화 조건에 대해 제시하고자 한다.

Keywords: 그래핀, 액정 섬유, 습식방사, 에너지 장치, 플렉서블 디바이스